

UNIVERSITY OF WARMIA AND MAZURY IN OLSZTYN

Technical Sciences

18(2) 2015



PUBLISHER UWM

Editorial Board

Ceslovas Aksamitauskas (Vilnius Gediminas Technical University, Lithuania), Stefan Cenkowski (University of Manitoba, Canada), Adam Chrzanowski (University of New Brunswick, Canada), Davide Ciucci (University of Milan-Bicocca, Italy), German Efremov (Moscow Open State University, Russia), Mariusz Figurski (Military University of Technology, Poland), Dorota Grejner-Brzezinska (The Ohio State University, USA), Janusz Laskowski (University of Life Sciences in Lublin, Poland), Lech Tadeusz Polkowski (Polish-Japanese Institute of Information Technology, Poland), Vladimir Tilipalov (Kaliningrad State Technical University, Russia), Alojzy Wasilewski (Koszalin University of Technology, Poland)

Editorial Committee

Marek Markowski (Editor-in-Chief), Piotr Artiemjew, Kamil Kowalczyk, Wojciech Sobieski, Piotr Srokosz, Magdalena Zielińska (Assistant Editor), Marcin Zieliński

Features Editors

Piotr Artiemjew (Information Technology), Marcin Dębowski (Environmental Engineering), Marek Mróz (Geodesy and Cartography), Ryszard Myhan (Biosystems Engineering), Wojciech Sobieski (Mechanical Engineering), Piotr Srokosz (Civil Engineering), Jędrzej Trajer (Production Engineering)

Statistical Editor
Paweł Drozda

Executive Editor
Mariola Jezierska

The Technical Sciences is indexed and abstracted in BazTech (<http://baztech.icm.edu.pl>) and in IC Journal Master List (<http://journals.indexcopernicus.com>)

The Journal is also available in electronic form on the web sites
<http://www.uwm.edu.pl/techsci> (subpage Issues)
<http://wydawnictwo.uwm.edu.pl> (subpage Czytelnia)

The print edition is the primary version of the Journal

PL ISSN 1505-4675

© Copyright by Wydawnictwo UWM • Olsztyn 2015

Address

ul. Jana Heweliusza 14
10-718 Olsztyn-Kortowo, Poland
tel.: +48 89 523 36 61
fax: +48 89 523 34 38
e-mail: wydawca@uwm.edu.pl

Contents

Biosystem Engineering

K.W. NOWAK – <i>Identification of Meat Types by Ultrasonic Methods</i>	79
Z. KALINIEWICZ, P. MARKOWSKI, A. ANDERS, K. JADWISIENČZAK – <i>Frictional Properties of Selected Seeds</i>	85

Civil Engineering

B.M. DEJA, J. TYBURSKI – <i>Selected Aspects of Designing and Realization of Low Energy Single-Family Houses According to the NF15 and NF40 Standards</i> . .	103
---	-----

Environmental Engineering

D. KARDAŚ, J. KLUSKA, J. SZUSZKIEWICZ, M. SZUMOWSKI – <i>Experimental Study of Thermal Pyrolysis of Turkey Feathers</i>	115
J. LEŚNY, M. PANFIL, M. URBANIAK, R. SCHEFKE – <i>Examining Technical Solutions for a Prototype of a Solar-Air Collector</i>	125

Geodesy and Cartography

Z. SZCZEPANIAK-KOŁTUN – <i>Use of Lidar Data and Selected Algorithms for Determining the Flow Lines</i>	137
---	-----

IDENTIFICATION OF MEAT TYPES BY ULTRASONIC METHODS

Konrad W. Nowak

Department of Systems Engineering
University of Warmia and Mazury in Olsztyn

Received 31 July 2014; accepted 3 February 2015; available on line 7 February 2015.

Key words: ultrasonics, sound velocity, meat, identification.

Abstract

The ability of identification of meat types using ultrasonic measurement was evaluated in this work. Four types of muscles were analyzed (turkey breast and thigh, and pork loin and ham). Ultrasonic measurements were performed at storage ($5 \pm 1^\circ\text{C}$) and room ($20 \pm 1^\circ\text{C}$) temperatures using the through-transmission technique and differential method of determination of sound velocity and the attenuation coefficient. The mean values of sound velocity for the breast, thigh, loin and ham were respectively: 1550.7, 1536.6, 1558.7, 1559.7 m/s at the storage temperature, and 1582.7, 1578.5, 1596.9, 1592.7 m/s at the room temperature. The mean values of the attenuation coefficient in the same order were: 21.3, 23.2, 30.6, 28.1 m^{-1} and 22.2, 18.9, 22.0, 22.4 m^{-1} . Statistically significant differences in the sound velocity were observed between pork and turkey muscles, therefore, the meat of those species can be identified based on ultrasound measurements of sound velocity. The attenuation coefficient cannot be applied in the identification of meat types due to absence of significant differences in the mean values.

Symbols:

A – amplitude of registered ultrasound signal, mV,
 c – sound velocity, m/s,
 d – distance between transducers (sample thickness), m,
 α – acoustic attenuation coefficient, m^{-1} ,
 t – temperature, $^\circ\text{C}$,
 τ – time, μs .

Introduction

Cases in which food producers adulterate the composition of their products, intentionally or not, are well known. Some manufacturers cheat by adding or substituting ingredients in food products for cheaper ones to earn more profits (MOORE et al. 2012). Such illegal practices are also noted in the meat

processing. In a recent publicized case, undeclared horse meat was added to meat products (PREMANANDH 2013). Whereas, the identification of the origins of meat is of great importance due to public health, legal and economic concerns as well as religious and ethical considerations (AMARAL et al. 2014).

Several modern techniques allow to identify meat type or some additives used in meat production. They include measurements of stable isotope ratios, histology and image analysis, spectroscopy, metabolomics and polymerase chain reaction assays, which have been described in detail by SENTANDREU and SENTANDREU (2014). Despite numerous advantages, the above methods share a common disadvantage: they require sophisticated equipment, which makes them comparatively expensive. However, the authentication of meat products should be used as a screening test that is fast, relatively cheap, nondestructive, and uses equipment that is compact and portable. Ultrasonic methods, which are used in the identification of other food products, such as honey (RATAJSKI et al. 2010), offer such capabilities.

A method for determining the composition of biological materials based on the velocity of sound waves penetrating that material is well known (GHAEDIAN et al. 1998, BENEDITO et al. 2001). A research hypothesis was formulated that the above method could be used to determine the proportions of raw meat (muscles of different origins of animals) in a meat product or to verify whether a product contains the raw materials declared by the manufacturer. But it could be possible only if significant differences in sound velocity are observed between ingredients. Therefore, the objective of this study was to evaluate the usefulness of ultrasonic measurements in differentiating various types of meat (e.g. poultry from pork) and muscles using sound velocity.

Materials and Methods

Four types of muscles were used in this study: pork loin (*m. longissimus dorsi*), pork ham (*m. biceps femoris*), turkey breast (*m. pectoralis major*) and turkey thigh (*m. extensor iliotibialis*). Every type of meat was represented by 30 samples, each obtained from a different animal. The muscles were analyzed 48 hours *post mortem*. They were regarded as food rather than living tissue, therefore, they were not de-aired.

Ultrasonic measurements were performed at storage temperature ($5 \pm 1^\circ\text{C}$) and room temperature ($20 \pm 1^\circ\text{C}$). The signals were acquired by the through-transmission (TT) technique perpendicular to muscle fibers. The experimental stand consisted of the OPBOX 2.0 acoustic pulser-receiver (PBP Optel, Poland) and transducers with nominal frequency of 2 MHz (PBP Optel, Poland). The experimental set up is shown in Figure 1.

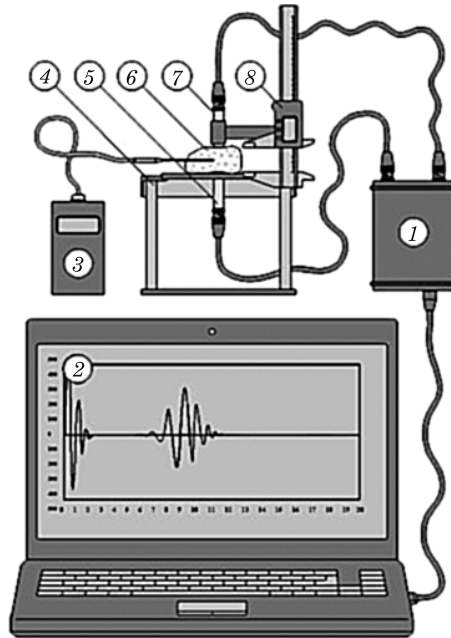


Fig. 1. Experimental stand: 1 – OPBOX 2.0, 2 – PC, 3 – electronic thermometer, 4 – platform, 5 – fixed acoustic transducer, 6 – sample, 7 – movable acoustic transducer, 8 – electronic caliper

Sound velocity was determined by the differential method (using two samples of the same material with different thickness) (NOWAK, MARKOWSKI 2013) based on Equation 1, where: d_1 and d_2 are thicknesses of thick and thin samples; τ_1 and τ_2 are time of flight (in this case, time when the received signal reaches maximum amplitude).

$$c = \frac{d_2 - d_1}{\tau_2 - \tau_1} \quad (1)$$

The attenuation coefficient was determined based on Equation 2.

$$\alpha = \frac{1}{d_2 - d_1} \ln \frac{A_1}{A_2} \quad (2)$$

The results were processed using one-way analysis of variance (ANOVA) and the Kruskal-Wallis nonparametric test at the significance level of $p = 0.05$. The Kruskal-Wallis test was chosen because the variances were hetero-

geneous. Data were processed in the STATISTICA 10.0 package (Stat Soft Inc., USA). The mean values of sound velocity, attenuation coefficient and the results of the statistical analysis are shown in Table 1. The correlations between the results are presented in Figure 2.

Table 1
Mean values of sound velocity and the attenuation coefficient in the analyzed muscles (standard deviation values are given in brackets)

Muscle	Sound velocity c [m/s]*		Attenuation coefficient α [1/m]*	
	$t = 5 \pm 1^\circ\text{C}$	$t = 20 \pm 1^\circ\text{C}$	$t = 5 \pm 1^\circ\text{C}$	$t = 20 \pm 1^\circ\text{C}$
	Turkey breast (<i>m. pectoralis major</i>)	1550.7 (5.4) ^A	1582.7 (6.3) ^A	21.3 (10.4) ^A
Turkey thigh (<i>m. extensor iliotalibialis</i>)	1536.6 (8.6) ^B	1578.5 (5.7) ^A	23.2 (11.7) ^{A,B}	18.9 (7.7) ^A
Pork loin (<i>m. longissimus dorsi</i>)	1558.7 (8.5) ^C	1596.9 (4.7) ^B	30.6 (13.0) ^B	22.0 (9.4) ^A
Pork ham (<i>m. biceps femoris</i>)	1559.7 (5.5) ^C	1592.7 (5.9) ^B	28.1 (13.4) ^{A,B}	22.4 (12.1) ^A

* Values in the same column marked with different letters are statistically different ($p=0.05$).

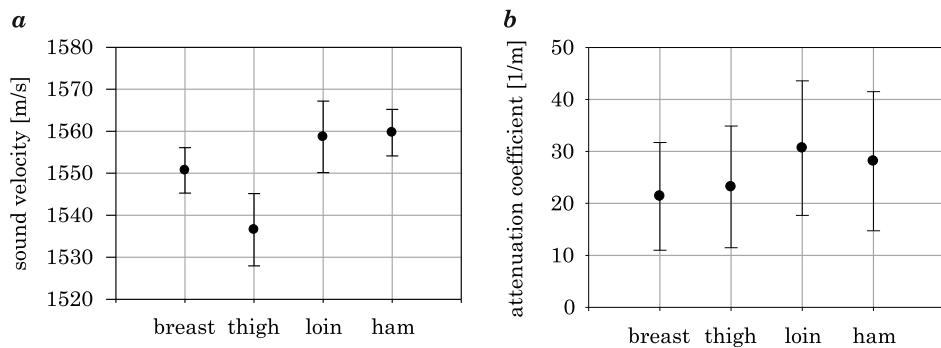


Fig. 2. Sound velocity and attenuation coefficients in the analyzed turkey and pork muscles at storage temperature ($5 \pm 1^\circ\text{C}$)

Results and Discussion

The mean values of the determined parameters and the results of the statistical analysis are presented in Table 1. Sound velocity in pork loin (*m. longissimus dorsi*) was similar to that reported in a different study (NOWAK, MARKOWSKI 2013) where it reached 1557.4 m/s at storage temperature and 1598.3 m/s at room temperature. At near room temperature ($24 \pm 0.5^\circ\text{C}$), sound velocity for the above muscle was determined at 1601.4 by SARVAZYAN et al. (2005). At room temperature, sound velocity in turkey breast was somewhat higher than that determined by GLOZMAN and AZHARI (2010) at 1576.3, but in

the cited study, the muscles had been prepared to be as homogenous as possible, which probably resulted in lower sound velocity values. The above authors described the measurement technique, but failed to indicate the method of determining sound velocity (in particular time of flight). Whereas, the choice of method for determination of sound velocity based on the received acoustic signal can significantly underestimate the results (NOWAK, MARKOWSKI 2013).

Significant differences between mean values of sound velocity were noted in turkey muscles at storage temperature, and the observed values differed significantly from the relevant results in both pork muscles. The mean values of sound velocity did not differ significantly between pork muscles. At room temperature, no statistically significant differences in mean sound velocity values were found in the group of the analyzed turkey muscles or in the group of the evaluated pork muscles, but significant differences were observed between those groups. The above indicates that turkey muscles differ significantly from pork muscles in sound velocity regardless of temperature.

Taking into account the mean values of the attenuation coefficient at storage temperature, groups of turkey muscles and pork muscles did not differ significantly. No significant differences in the values of the attenuation coefficient were noted between turkey breast and turkey thigh, or between turkey thigh vs. pork loin and pork ham. There was a general absence of significant differences in the attenuation coefficient at room temperature.

Temperature seems to play a key role in the identification of meat types based on sound velocity. In this study 5°C increase in the temperature of a meat sample increased mean sound velocity by about 10 m/s, whereas the differences in mean sound velocity of turkey breast and both pork muscles were below 10 m/s. The above suggests that inaccurate temperature measurements can be largely responsible for errors in the future identification of meat from different animal species using sound velocity.

Conclusions

Statistically significant differences in the sound velocity were observed between pork muscles and turkey muscles, therefore, the meat from these two species can be identified based on the results of ultrasound measurements, in particular measurements of sound velocity. It should be noted that inaccurate temperature measurement and sound velocity determination can undermine the reliability of such identification of product ingredients.

The attenuation coefficient was not effective in differentiating meat types due to high standard deviation and the resulting absence of significant

differences in the mean values of the attenuation coefficient describing the muscles of different species.

Further research is needed to evaluate the meat of other species (e.g. beef and chicken) and measure sound velocity in muscles that have been blended, mixed and thermally processed.

Acknowledgements

This study was supported by grant N N313 789140 from the Polish Ministry of Science and Higher Education.

References

- AMARAL J.S., SANTOS C.G., MELO V.S., OLIVEIRA M.B.P.P., MAFRA I. 2014. *Authentication of a traditional game meat sausage (Alheira) by species-specific PCR assays to detect hare, rabbit, red deer, pork and cow meats*. Food Research International, 60: 140–145.
- BENEDITO J., CARCEL J.A., ROSSELLO C., MULET A. 2001. *Composition assessment of raw meat mixtures using ultrasonics*. Meat Science, 57: 365–370.
- GHAEDIAN R., COUPLAND J.N., DECKER E.A., MCCLEMENTS D.J. 1998. *Ultrasonic determination of fish composition*. Journal of Food Engineering, 35: 323–337.
- GLOZMAN T., AZHARI H. 2010. *A method for characterization of tissue elastic properties combining ultrasonic computed tomography with elastography*. Journal of Ultrasound in Medicine, 29: 387–398.
- MOORE J.C., SPINK J., LIPP M. 2012. *Development and application of a database of food ingredient fraud and economically motivated adulteration from 1980 to 2010*. Journal of Food Science, 77(4): R118–R126.
- NOWAK K.W., MARKOWSKI M. 2013. *A comparison of methods for the determination of sound velocity in biological materials: A case study*. Ultrasonics, 53(5): 923–927.
- PREMANANDH J. 2013. *Horse meat scandal – A wake-up call for regulatory authorities*. Food Control, 34: 568–569.
- RATAJSKI A., BIAŁOBRZEWSKI I., DAJNOWIEC F., BAKIER S. 2010. *The use of ultrasonic methods in the identification of honey types*. Technical Sciences, 13: 22–29.
- SARVAZYAN A., TATARINOV A., SARVAZYAN N. 2005. *Ultrasonic assessment of tissue hydration status*. Ultrasonics, 43: 661–671.
- SENTANDREU M.A., SENTANDREU E. 2014. *Authenticity of meat products: Tools against fraud*. Food Research International, 60: 19–29.

FRictional PROPERTIES OF SELECTED SEEDS

*Zdzisław Kaliniewicz, Piotr Markowski, Andrzej Anders,
Krzysztof Jadwisieńczyk*

Department of Heavy Duty Machines and Research Methodology
University of Warmia and Mazury in Olsztyn, Poland

Received 31 August 2014; accepted 12 March 2015; available on line 19 March 2015.

Key words: physical attributes, coefficient of external friction, relation.

Abstract

The thickness, width, length and weight of five seed species (buckwheat, vetch, pea, lupine and faba bean) and their external friction angle were determined on two types of surfaces – steel and rubber. The experiment was performed with the use of an inclined plane with an adjustable angle of inclination that measures the angle of external friction and the time taken by seeds to travel a given distance, which supports the determination of the coefficient of kinetic friction. The measured parameters were used to calculate arithmetic and geometric mean diameter, aspect ratio and sphericity index. The dimensions, weight and the calculated indicators of the examined seeds did not significantly affect their coefficients of static and kinetic friction or their coefficients of rolling resistance and rolling friction. The studied parameters were largely influenced by the type of friction surface, and significantly lower average values were reported for steel than rubber. In the studied seed species, the static friction coefficient was determined in the range of 0.187 to 0.582, kinetic friction coefficient – 0.134 to 0.479, rolling resistance coefficient – 0.148 to 0.529 and rolling friction coefficient – 0.29 to 1.80 mm.

Symbols:

- D_a – arithmetic mean diameter, mm,
- D_g – geometric mean diameter, mm,
- m – seed weight, mg
- f_1, f_2 – coefficient of rolling friction of seeds on steel and rubber, respectively, mm,
- r – radius of a rolling seed, mm,
- R – aspect ratio, %,
- S – travel distance of the particle, m,
- t – time required by the particle to travel distance, s,
- T, W, L – seeds thickness, width and length, mm,
- x, SD – average value and standard deviation of trait,
- x_{\min}, x_{\max} – minimum and maximum value of trait,
- α – angle of external friction of seeds, °,
- α_{s1}, α_{s2} – angle of static friction of seeds on steel and rubber, respectively, °,
- α_{r1}, α_{r2} – angle of rolling friction of seeds on steel and rubber, respectively, °,
- μ – coefficient of external friction of seeds,

Correspondence: Zdzisław Kaliniewicz, Katedra Maszyn Roboczych i Metodologii Badań, Uniwersytet Warmińsko-Mazurski, ul. Oczapowskiego 11/B112, 10-719 Olsztyn, phone: +48 89 523 39 34, e-mail: zdzislaw.kaliniewicz@uwm.edu.pl

-
- μ_{k1}, μ_{k2} – coefficient of kinetic friction of seeds on steel and rubber, respectively,
 μ_{s1}, μ_{s2} – coefficient of static friction of seeds on steel and rubber, respectively,
 μ_{r1}, μ_{r2} – coefficient of rolling resistance of seeds on steel and rubber, respectively,
 Φ – sphericity index, %.

Introduction

A thorough understanding of frictional forces is required for analyzing and modeling various processes. The knowledge of frictional properties is essential for the selection of sowing, harvesting, transport, cleaning, sorting, storage and processing parameters of plant materials (HORABIK 2001, ALTUNTAS, DEMIRTOLA 2007, KABAS et al. 2007, KRAM 2008, RIYAHY et al. 2011, JOUKI, KHAZAEI 2012, SOLOGUBIK et al. 2013). Biological materials are characterized by morphological variation, and their frictional properties can differ significantly. An analysis of published sources (MOHSENIN 1986, HORABIK 2001, YALÇIN, ÖZARSLAN 2004, KRAM 2006, 2008, AFZALINIA, ROBERGE 2007, ALTUNTAS, DEMIRTOLA 2007, SHAROBEEM 2007, DAVIES, EL-OKENE 2009, IZLI et al. 2009, ŁUKASZUK et al. 2009, GHARIBZAHEDI et al. 2011, KALKAN, KARA 2011, TARIGHI et al. 2011) indicates that frictional parameters of plant materials are determined by species (variety), ripeness, moisture content, friction surface material, material porosity, velocity relative to the friction surface, orientation relative to the direction of motion, normal pressure exerted on particles, variations in particle shape and time of material storage.

Seeds can be cleaned and sorted with the use of a string sieve. The structure and geometric parameters of a string sieve have been discussed by the author in previous publications (KALINIEWICZ 2011, 2013a). Since separated seeds move along strings, and the width of openings between strings changes along the screen, possible correlations between the coefficient of external friction, dimensions and weight of seeds have to be investigated before the separation process is analyzed. In a study of principal cereal species (wheat, rye, barley, oats and triticale) (KALINIEWICZ 2013b), significant correlations were not observed between the above attributes. Conclusive information about the presence of such correlations in other species of seed-producing plants is not available in literature.

The objective of this study was to determine the variability in external friction coefficients of selected seed species and to identify the correlations between those parameters and the main physical attributes of seeds. The resulting data can be used to model industrial processes, in particular seed separation on a string sieve.

Materials and methods

The experimental material comprised buckwheat, vetch, pea, lupine and faba bean seeds obtained from three sources (Table 1): Potato and Seed Breeding Center in Olsztyn, a seed farm in Wodzierady and Department of Plant Breeding and Seed Production of the University of Warmia and Mazury in Olsztyn. Subject to species, the relative moisture content of seeds was decreased to 10.9–12.5% to enable long-term storage (KALETA, GÓRNICKI 2008, RUDZIŃSKI 2011).

Table 1
Experimental material

Seed species	Seed variety	Producer	Moisture content [%]
Buckwheat	Panda	Department of Plant Breeding and Seed Production of the University of Warmia and Mazury in Olsztyn	12.5
Vetch	Hanka	OLZNAS-CN Potato Breeding and Seed Production Center in Olsztyn	11.8
Pea	Eureka	GRANUM seed farm, J. Manias, S. Menc, J. Szymański Sp. j., Wodzierady	12.1
Lupin	Emir	OLZNAS-CN Potato Breeding and Seed Production Center in Olsztyn	11.5
Faba bean	Nadwiślański	OLZNAS-CN Potato Breeding and Seed Production Center in Olsztyn	10.9

A survey sampling method (GREŃ 1984) was used to randomly select 120 seeds representing every tested species. In the analyzed seed samples, the standard error of the mean did not exceed:

- for three basic seed dimensions – 0.1 mm (0.2 mm for faba bean),
- for the angle of external friction – 0.4° for buckwheat, lupine and faba bean, 0.6° for vetch, 0.8° for pea,
- for seed weight – 2 mg for buckwheat and vetch, 8 mg for pea and lupine, 24 mg for faba bean.

The length and width of seeds were determined with the accuracy of 0.02 mm under the MWM 2325 laboratory microscope, and seed thickness was measured using a dial indicator device with measurement precision of 0.01 mm. The above measurements were performed in accordance with the methodology described by KALINIEWICZ et al. (2011).

Seeds were weighed on WAA 100/C/2 laboratory scales with the accuracy of 0.1 mg.

The measured parameters were used to determine the arithmetic D_a and geometric mean diameter D_g , aspect ratio R and sphericity index Φ (MOHSENIN 1986):

$$D_a = \frac{T + W + L}{3} \quad (1)$$

$$D_g = (T \cdot W \cdot L)^{\frac{1}{3}} \quad (2)$$

$$R = \frac{W}{L} \cdot 100 \quad (3)$$

$$\Phi = \frac{(T \cdot W \cdot L)^{\frac{1}{3}}}{L} \cdot 100 \quad (4)$$

A flat friction plate with an adjustable angle of inclination was used in the study, therefore the coefficient of static friction μ (both the coefficient of sliding friction μ_s for seeds sliding on the surface, and the coefficient of rolling resistance μ_t for seeds rolling on the surface) of seeds was calculated from a universally applied formula (GROCHOWICZ 1994, MOLENDEN et al. 1995, KRAM 2006, YALÇIN et al. 2007, LAWROWSKI 2008, RAZAVI, FARAHMANDFAR 2008, RIYAHİ et al. 2011, TARIGHI et al. 2011, DARVISHI 2012, NOSAL 2012, SOLOGUBIK et al. 2013):

$$\mu = \tan \alpha \quad (5)$$

The angles of external friction at which seed motion was initiated through sliding or rolling were determined for each seed on two types of friction surfaces: steel and rubber. Surface porosity was described by parameter R_a measured by the Hommel Tester T1000 device. The average value of R_a was $0.48 \mu\text{m}$ for steel and $0.79 \mu\text{m}$ for rubber. The device and the method for measuring the angle of external friction were described by KALINIEWICZ (2013b). Seeds were placed with their longitudinal axis parallel to the inclined plane. The angle of inclination was measured with the precision of 0.01° , and seed travel time – with the precision of 1 ms. Due to irregular seed shape and the momentary detachment of seeds from the friction surface, the time of travel was determined only for sliding seeds. Having passed labile equilibrium (FRĄCZEK 1999), seeds move on the friction surface in sliding motion, rolling

motion or a combination of both. The analysis was performed only on seeds whose motion could be classified as typically sliding or rolling. For sliding seeds, the coefficient of kinetic friction was determined based on time t required for traveling the distance of $S = 140$ mm on a plane inclined at angle α_s (GROCHOWICZ 1994):

$$\mu_k = \tan \alpha_s - \frac{2S}{gt^2 \cos \alpha_s} \quad (6)$$

For rolling seeds, the coefficient of rolling friction f was calculated from the below equation (LAWROWSKI 2008, NOSAL 2012):

$$f = \mu_t \cdot r = r \cdot \tan \alpha_t \quad (7)$$

where r is the radius of a rolling seed. Based on the expected seed distribution on a given friction surface, it was assumed that radius represents the average half thickness and length of a given seed, and it equals:

$$r = \frac{T + L}{4} \quad (8)$$

The results were processed in the Statistica PL v. 10 application at the significance level of $\alpha = 0.05$. The differences in friction coefficients of the analyzed seed species on various friction surfaces were determined by ANOVA. The normality of each group was determined by the Shapiro-Wilk test, and the equality of variances was assessed with Levene's test. Where the null hypothesis of equal population means was rejected, multiple comparisons were performed post-hoc to examine the differences and identify homogenous groups with the use of Duncan's test. A correlation analysis was performed to determine the strength and direction of correlations between friction coefficients and physical parameters of seeds. The degrees of correlation were evaluated with the use of Pearson's correlation coefficients (RABIEJ 2012).

Results

The physical parameters of the analyzed seeds are presented in Table 2. The lowest width and thickness values were noted in buckwheat, and the highest – in faba bean. The latter species was also characterized by the highest average length. Vetch seeds were the shortest with average length of 4.4 mm. The seeds were also characterized by the smallest arithmetic and geometric mean diameter and the highest aspect ratio. The highest values of arithmetic

and geometric mean diameter were noted in faba bean, and the highest sphericity index was reported in pea seeds. The lowest average values of the aspect ratio and sphericity index were observed in buckwheat seeds.

The coefficient of external friction was determined upon the initiation of seed motion. The percentage share of seeds sliding or rolling on a given friction surface is given in Figure 1. All buckwheat seeds were characterized by sliding motion on both tested surfaces. An analysis of seed motion on friction surfaces revealed that significantly more seeds were set into motion by rolling on a rubber surface than on a steel surface. Pea seeds were most susceptible to rolling (approximately 62% on steel and approximately 88% on rubber). The susceptibility of the remaining seed species was determined by the type of friction surface.

Table 2

Statistical parameters of physical attributes of seeds

Parameter	Seed species				
	buckwheat $x \pm SD$	vetch $x \pm SD$	pea $x \pm SD$	lupin $x \pm SD$	faba bean $x \pm SD$
m	24.9 ± 4.92	44.1 ± 9.38	249.2 ± 43.68	171.8 ± 30.47	478.2 ± 132.02
T	3.6 ± 0.25	3.3 ± 0.30	6.2 ± 0.45	5.2 ± 0.34	7.4 ± 0.72
W	4.1 ± 0.30	4.2 ± 0.29	7.0 ± 0.51	6.3 ± 0.44	8.5 ± 0.85
L	6.0 ± 0.53	4.4 ± 0.32	7.6 ± 0.48	7.5 ± 0.53	10.2 ± 1.12
D_a	4.6 ± 0.28	4.0 ± 0.27	7.0 ± 0.42	6.3 ± 0.38	8.7 ± 0.83
D_g	4.4 ± 0.27	3.9 ± 0.27	6.9 ± 0.42	6.3 ± 0.37	8.6 ± 0.82
R	69.0 ± 6.54	94.0 ± 3.73	92.4 ± 4.57	84.0 ± 4.43	84.2 ± 5.47
ϕ	74.7 ± 4.83	88.9 ± 2.93	91.3 ± 2.76	83.3 ± 2.62	85.1 ± 3.81

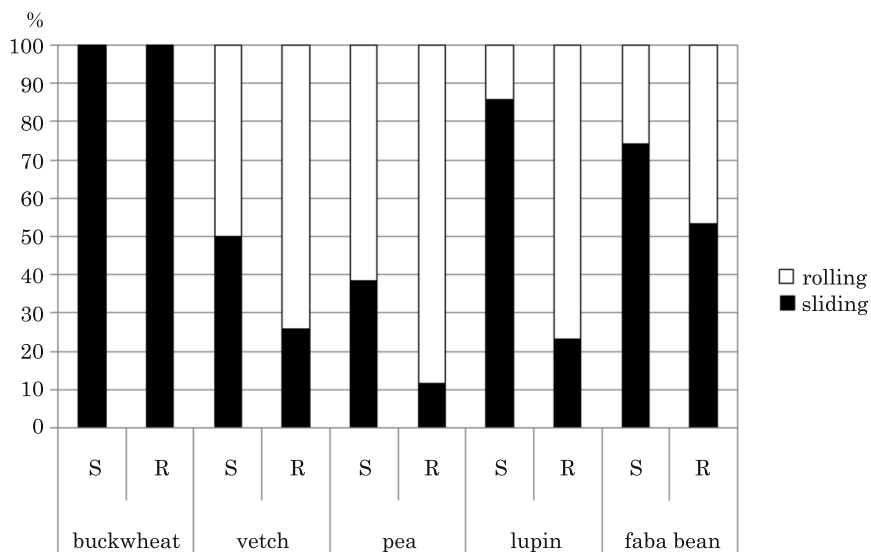


Fig. 1. Percentage share of seeds sliding or rolling on a given friction surface: S – steel, R – rubber

The coefficients of static friction (Table 3) of the analyzed seeds ranged from 0.187 (faba bean) to 0.426 (vetch) on steel, and from 0.267 (faba bean) to 0.582 (buckwheat) on rubber. Based on the average values of the coefficient of static friction on a steel surface, the analyzed species were sorted in the following rising sequence: faba bean (0.220), lupine (0.281), vetch (0.297), buckwheat (0.315) and pea (0.339). The average values of the coefficient of static friction on a rubber surface were determined in the range of 0.327 (faba bean) to 0.465 (buckwheat). No significant differences in the average values of the coefficient of static friction were observed between buckwheat and pea seeds or between vetch and lupine seeds. The greatest variations in the coefficient of rolling resistance on steel were reported for vetch (from 0.148 to 0.378). The studied seed species were arranged in the following rising sequence based on the average values of the coefficient of rolling resistance: faba bean (0.198), lupine (0.252), vetch (0.259) and pea (0.286). No significant differences in the average values of the coefficient of rolling resistance were noted between vetch and lupine. On a rubber surface, the coefficient of rolling resistance ranged from 0.170 (faba bean) to 0.529 (pea). Faba bean and pea were also

Table 3
Statistical distribution of the coefficients of static friction and the coefficients of rolling resistance of the analyzed seeds

Seed species	Coefficient of friction	x_{\min}	x_{\max}	x	SD
Buckwheat	μ_{s1}	0.218	0.419	0.315 ^{Da}	0.041
	μ_{s2}	0.375	0.582	0.465 ^{Cb}	0.042
Vetch	μ_{s1}	0.228	0.426	0.297 ^{Ca}	0.042
	μ_{s2}	0.314	0.459	0.381 ^{Bb}	0.036
	μ_{r1}	0.148	0.378	0.259 ^{Ba}	0.048
	μ_{r2}	0.178	0.482	0.312 ^{Bb}	0.061
Pea	μ_{s1}	0.286	0.418	0.339 ^{Ea}	0.031
	μ_{s2}	0.372	0.559	0.460 ^{Cb}	0.053
	μ_{r1}	0.183	0.369	0.286 ^{Ca}	0.041
	μ_{r2}	0.182	0.529	0.353 ^{Cb}	0.077
Lupin	μ_{s1}	0.227	0.364	0.281 ^{Ba}	0.028
	μ_{s2}	0.333	0.455	0.386 ^{Bb}	0.030
	μ_{r1}	0.199	0.305	0.252 ^{Ba}	0.026
	μ_{r2}	0.255	0.434	0.344 ^{Cb}	0.037
Faba bean	μ_{s1}	0.187	0.358	0.220 ^{Aa}	0.025
	μ_{s2}	0.267	0.385	0.327 ^{Ab}	0.032
	μ_{r1}	0.155	0.242	0.198 ^{Aa}	0.018
	μ_{r2}	0.170	0.376	0.277 ^{Ab}	0.042

A, B, C, D, E – different letters in the superscript represent statistically significant differences between seeds of different species

a, b – different letters in the superscript represent statistically significant differences between friction surfaces

characterized by the lowest and highest average values of the coefficient of rolling resistance at 0.277 and 0.353, respectively. Similar average values of the above coefficient were reported for pea and lupine. In a comparison of the coefficient of external friction, significant differences in average object values were observed for the analyzed friction surfaces as well as for sliding and rolling motion of every seed species. Lower values of the coefficient of external friction were reported for the steel surface and rolling motion.

Similarly to the coefficient of static friction, lower values of the coefficient of kinetic friction were reported on a steel surface (Table 4). The lowest values of the coefficient of kinetic friction were determined for faba bean on both tested surfaces. The highest average value of the above coefficient was observed for pea (steel) and buckwheat (rubber). No significant differences in the average values of the coefficient of kinetic friction were reported between vetch and lupine on both friction surfaces.

The coefficient of rolling friction ranged from 0.29 mm (vetch) to 1.34 mm (pea) on a steel surface, and from 0.33 mm (vetch) to 1.80 mm (pea and lupine)

Table 4
Statistical distribution of the coefficients of kinetic friction and the coefficients of rolling friction of the analyzed seeds

Seed species	Coefficient of friction	x_{\min}	x_{\max}	x	SD
Buckwheat	μ_{k1}	0.164	0.314	0.233 ^{Ca}	0.033
	μ_{k2}	0.213	0.479	0.346 ^{Db}	0.049
Vetch	μ_{k1}	0.140	0.319	0.217 ^{Ba}	0.034
	μ_{k2}	0.198	0.344	0.262 ^{Bb}	0.032
	f_1	0.29	0.76	0.51 ^{Aa}	0.10
	f_2	0.33	0.97	0.60 ^{Ab}	0.13
Pea	μ_{k1}	0.185	0.336	0.262 ^{Da}	0.032
	μ_{k2}	0.134	0.368	0.286 ^{Cb}	0.071
	f_1	0.63	1.34	0.99 ^{Da}	0.14
	f_2	0.68	1.80	1.22 ^{Cb}	0.26
Lupin	μ_{k1}	0.156	0.286	0.220 ^{Ba}	0.024
	μ_{k2}	0.187	0.355	0.264 ^{Bb}	0.038
	f_1	0.56	0.96	0.78 ^{Ba}	0.10
	f_2	0.78	1.42	1.09 ^{Bb}	0.15
Faba bean	μ_{k1}	0.145	0.234	0.198 ^{Aa}	0.014
	μ_{k2}	0.148	0.284	0.221 ^{Ab}	0.028
	f_1	0.64	1.09	0.85 ^{Ca}	0.11
	f_2	0.73	1.80	1.21 ^{Cb}	0.22

A, B, C, D – different letters in the superscript represent statistically significant differences between seeds of different species

a, b – different letters in the superscript represent statistically significant differences between friction surfaces

on a rubber surface. Statistically equal average values were noted only for pea and faba bean seeds moving on a rubber surface.

An analysis of the data presented in Table 5 suggests that the analyzed physical attributes (weight, dimensions and the calculated indicators) were weakly correlated with friction coefficients. The smallest number of significant correlations with friction coefficients was noted for the coefficient of proportionality (5 out of 36 comparisons), and the highest – for seed weight (15 out of

Table 5
Pearson's coefficients of correlation between external friction coefficients and the remaining physical parameters of seeds

Seed species		m	T	W	L	D_a	D_g	R	Φ
Buckwheat	μ_{s1}	-0.39	-0.08	0.12	0.09	0.08	0.07	-0.02	-0.08
	μ_{s2}	-0.22	-0.04	0.03	-0.19	-0.12	-0.09	0.21	0.17
	μ_{k1}	-0.21	-0.02	0.05	0.18	0.13	0.10	-0.14	-0.16
	μ_{k2}	-0.20	0.06	0.17	0.19	0.20	0.19	-0.06	-0.10
Vetch	μ_{s1}	-0.15	-0.24	-0.10	-0.13	-0.17	-0.18	0.09	-0.08
	μ_{s2}	-0.14	-0.13	-0.16	-0.27	-0.21	-0.21	0.26	0.19
	μ_{k1}	0.27	0.15	0.25	0.38	0.31	0.31	-0.27	-0.26
	μ_{k2}	-0.21	-0.41	0.02	0.08	-0.09	-0.14	-0.12	-0.48
	μ_{r1}	-0.16	-0.19	-0.01	-0.09	-0.10	-0.11	0.15	-0.03
	μ_{r2}	-0.09	-0.23	0.06	0.15	-0.01	-0.03	-0.15	-0.42
	f_1	0.20	0.16	0.30	0.27	0.26	0.26	0.08	-0.06
	f_2	0.24	0.09	0.34	0.45	0.33	0.31	-0.21	-0.37
Pea	μ_{s1}	-0.30	-0.31	-0.40	-0.39	-0.41	-0.40	-0.14	-0.07
	μ_{s2}	-0.03	0.08	0.02	0.14	0.09	0.09	-0.14	-0.11
	μ_{k1}	-0.19	-0.23	-0.36	-0.27	-0.32	-0.32	-0.23	-0.13
	μ_{k2}	0.42	0.44	0.48	0.16	0.38	0.39	0.45	0.43
	μ_{r1}	-0.26	-0.29	-0.29	-0.16	-0.27	-0.28	-0.21	-0.23
	μ_{r2}	-0.16	-0.31	-0.16	-0.06	-0.20	-0.21	-0.17	-0.31
	f_1	0.12	0.08	0.01	0.22	0.11	0.11	-0.27	-0.29
	f_2	0.09	-0.07	0.04	0.19	0.06	0.05	-0.17	-0.29
Lupin	μ_{s1}	-0.17	-0.32	-0.10	-0.05	-0.16	-0.18	-0.07	-0.25
	μ_{s2}	-0.19	-0.16	-0.11	-0.10	-0.14	-0.14	0.01	-0.03
	μ_{k1}	0.20	0.20	0.14	0.15	0.18	0.19	-0.01	0.05
	μ_{k2}	-0.31	-0.19	-0.33	-0.24	-0.30	-0.30	-0.11	-0.04
	μ_{r1}	0.36	0.07	0.50	0.43	0.42	0.41	0.19	-0.17
	μ_{r2}	0.16	-0.09	0.09	0.34	0.16	0.14	-0.32	-0.60
	f_1	0.71	0.46	0.67	0.77	0.74	0.73	0.05	-0.30
	f_2	0.60	0.38	0.44	0.74	0.60	0.58	-0.40	-0.64
Faba bean	μ_{s1}	0.09	0.11	0.11	0.09	0.11	0.11	-0.01	-0.01
	μ_{s2}	0.25	0.21	0.13	0.27	0.22	0.22	-0.22	-0.17
	μ_{k1}	0.33	0.32	0.32	0.30	0.34	0.34	-0.03	-0.02
	μ_{k2}	-0.09	-0.13	-0.05	-0.07	-0.09	-0.09	0.03	-0.03
	μ_{r1}	-0.05	-0.12	-0.01	0.13	0.01	-0.01	-0.26	-0.40
	μ_{r2}	0.05	-0.12	0.15	0.13	0.07	0.06	0.04	-0.25
	f_1	0.68	0.60	0.64	0.79	0.72	0.71	-0.22	-0.30
	f_2	0.56	0.39	0.61	0.62	0.58	0.57	-0.11	-0.39

Bold font indicates that the correlation coefficient has exceeded critical value

36 comparisons). In the dimensions, frictional properties were most significantly correlated with seed length (14 out of 36 comparisons). The highest number of significant correlations with the remaining physical attributes was observed for the coefficient of rolling friction of lupine (8 out of 8 comparisons), faba beans (7 out of 8 comparisons) and vetch (6 out of 8 comparisons) on a rubber surface. The use of other, non-linear correlation models did not lead to a significant increase in the values of correlation coefficients, which indicates that the analyzed traits and the calculated coefficients had a minor influence on the seeds' frictional properties.

The coefficients of static and kinetic friction were significantly correlated in only 6 out of 30 cases (Table 6). A low number of significant correlations and the variability in the signs of correlation coefficients testify to an absence of correlations between the analyzed friction coefficients. The use of other correlation models did not lead to major improvement in the analyzed parameters either.

Table 6
Coefficients of linear correlation describing the relationship between coefficients of static and kinetic friction

Seed species		μ_{s2}	μ_{k1}	μ_{k2}
Buckwheat	μ_{s1}	0.129	0.053	0.239
	μ_{s2}	1	0.088	0.094
	μ_{k1}		1	0.322
Vetch	μ_{s1}	0.605	-0.250	0.202
	μ_{s2}	1	-0.191	-0.065
	μ_{k1}		1	0.244
Pea	μ_{s1}	-0.078	0.360	0.005
	μ_{s2}	1	0.021	-0.478
	μ_{k1}		1	-0.211
Lupin	μ_{s1}	0.123	-0.383	0.071
	μ_{s2}	1	0.057	-0.078
	μ_{k1}		1	-0.240
Faba bean	μ_{s1}	0.081	0.054	0.141
	μ_{s2}	1	-0.016	-0.400
	μ_{k1}		1	0.023

Bold font indicates that the correlation coefficient has exceeded critical value

In most comparisons, significant correlations were noted between the coefficients of rolling resistance and rolling friction (Table 7). The critical value of the linear correlation coefficient was not exceeded only in three cases, all of which involved the same seed species (faba bean), which implies that the analyzed correlation coefficients were not statistically significant at the adopted level of significance. The strongest correlations were observed between coefficients of rolling resistance and rolling friction of seeds moving on a given surface.

Table 7
Coefficients of linear correlation describing the relationship between coefficients of rolling resistance and rolling friction

Seed species		μ_{r2}	f_1	f_2
Vetch	μ_{r1}	0.378	0.928	0.308
	μ_{r2}	1	0.372	0.940
	f_1		1	0.426
Pea	μ_{r1}	0.585	0.916	0.519
	μ_{r2}	1	0.545	0.960
	f_1		1	0.587
Lupin	μ_{r1}	0.659	0.904	0.659
	μ_{r2}	1	0.629	0.878
	f_1		1	0.793
Faba bean	μ_{r1}	0.362	0.693	0.342
	μ_{r2}	1	0.269	0.848
	f_1		1	0.612

Bold font indicates that the correlation coefficient has exceeded critical value

Discussion

The lowest sphericity index value was reported for buckwheat seeds, and the highest – for pea, which suggests that the above seeds were least and most likely to resemble a sphere, respectively. The above was validated by the percentage share of seeds whose motion on a given surface was initiated by rolling (Figure 1). The only exception were lupine seeds on rubber, where approximately 77% of seeds rolled on a rubber surface (only 14% on a steel surface). The above could be due to similarities in the porosity of the rubber surface and the surface of lupine seeds. According to MOLENDÁ et al. (1995), ŠLIPEK et al. (1999) and HORABIK (2001), the greatest changes in the coefficient of external friction induced by adhesive bonding are observed when the irregularities in the height of the friction surface change within a range of values similar to the irregularities in the height of grain surface. This friction pair is characterized by a high coefficient of sliding friction, therefore, after overcoming inertia, seeds initiate their motion mainly by rolling.

The reported values of the coefficient of static friction of pea seeds are somewhat higher than those noted by YALÇIN et al. (2007) and similar to those given by ALTUNTAS and DEMIRTOLA (2007). KRAM (2008) reported similar values of the analyzed coefficient for lupine seeds cv. Radames and somewhat smaller values for lupine seeds cv. Bar on a steel surface. FIROUZI et al. (2012) reported similar average values of the coefficient of static friction of faba bean and SHOUGHY and AMER (2006) observed significantly higher average values (from 0.24 to 0.30) than those noted in this study. With regard to vetch seeds,

YALÇIN and ÖZARSLAN (2004) reported somewhat lower values of the analyzed coefficient, whereas higher values were noted by TASER et al. (2005). The observed differences could be attributed to varietal differences as well as differences in growing conditions of the analyzed seed species. The observed differences in surface porosity across varieties can affect the values of the coefficient of friction (MOLENDNA et al. 1995, FRĄCZEK 1999, HORABIK 2001). The variations in species-specific values of the coefficient of sliding friction can also be attributed to differences in the geometric structure of friction surfaces. The vast majority of published studies fail to characterize the applied friction surfaces (e.g. porosity parameters), therefore, their results are difficult to compare with our findings. The similarities in the values of the coefficient of static friction between the seeds evaluated in this study and other seed species are given in Table 8.

Tabela 8

Similarities in the values of coefficients of static friction between the analyzed seeds and other seed species

Seed species	Coefficient of static friction	Similar seed species
Buckwheat	$\mu_{s1}=0.315 \pm 0.041$ $\mu_{s2}=0.465 \pm 0.042$	triticale (KRAM 2006) wheat (KRAM 2006, BOAC et al. 2010, KALINIEWICZ 2013b) rye (KRAM 2006, KALINIEWICZ 2013b) cowpea (KABAS et al. 2007)
Pea	$\mu_{s1}=0.339 \pm 0.031$ $\mu_{s2}=0.460 \pm 0.053$	barley (BOAC et al. 2010, KALINIEWICZ 2013b) oats (BOAC et al. 2010, KALINIEWICZ 2013b) castor (GHARIBZAHEDI et al. 2011) sandbox (IDOWU et al. 2012) hemp (TAHERI-GARAVAND et al. 2012)
Vetch	$\mu_{s1}=0.297 \pm 0.042$ $\mu_{s2}=0.381 \pm 0.036$	cowpea (YALÇIN 2007) lentil (BAGHERPOUR et al. 2010)
Lupin	$\mu_{s1}=0.281 \pm 0.028$ $\mu_{s2}=0.386 \pm 0.030$	canola (BOAC et al. 2010) black grape (KILIÇKAN et al. 2010) barley (SOLOGUBIK et al. 2013)
Faba bean	$\mu_{s1}=0.220 \pm 0.025$ $\mu_{s2}=0.327 \pm 0.032$	melon (SHIESHAA et al. 2007) soybean (KIBAR, ÖZTÜRK 2008) <i>Jatropha curcas</i> (KARAJ, MÜLLER 2010)

The values of the coefficient of rolling resistance are always lower than the values of the coefficient of static friction of seeds whose motion is initiated by sliding, and smaller differences were observed on a steel surface. The differences in the values of the above coefficients ranged from 10% (faba bean) to approximately 16% (pea) on steel, and from approximately 11% (lupine) to approximately 23% (pea) on rubber.

The values of the coefficient of kinetic friction were similar for pea moving on a steel surface and significantly lower for pea moving on a rubber surface in comparison with those reported by ALTUNTAS and DEMIRTOLA (2007). SHAROBEEM (2007) observed significantly higher values of the kinetic friction coefficient for faba bean on both steel and rubber surfaces. The above can be attributed to the use of various friction surface materials and the resulting differences in their porosity. The results presented by KALINIEWICZ (2013b) indicate that lupine and wheat seeds have similar average values of the coefficient of kinetic friction on both friction surfaces. Therefore, it can be assumed that those seeds are characterized by similar surface porosity and microhardness. The similarities in the values of the coefficient of kinetic friction between faba bean and rye seeds and between lupine and barley seeds on a steel surface and between pea seeds vs. rye and barley seeds on a rubber surface are not easy to explain because the components of the molecular-mechanical model of friction, developed by KRAGIELSKI and discussed by MOLEND A et al. (1995), FRĄCZEK (1999), ŚLIPEK et al. (1999) and HORABIK (2001), were not measured. The above could be attributed to similar relations between state of friction surfaces, seed microhardness and the actual area of contact between the seed and the friction surface. The value of the coefficient of kinetic friction of faba bean moving on steel is also comparable to that reported for safflower seeds (KARA et al. 2012).

A comparison of the coefficients of static and kinetic friction of the analyzed seeds indicates that the latter parameter is always lower, and it accounts from 62% to 90% of the value of the static friction coefficient. The observed decrease in the value of the coefficient of kinetic friction relative to the coefficient of static friction could be explained by the rapid drop in friction force after macro-sliding, which was observed by FRĄCZEK (1999). The authors agree with Frączek that the above results from the system's inertia, which is why the force required to initiate motion is much greater than the force required for its continuation. In this study, greater differences were noted on a rubber surface in most cases (excluding buckwheat). The above could be attributed to somewhat higher porosity of the rubber surface relative to the steel surface as well as lower hardness of the rubber surface.

The dimensions, weight and shape factors of seeds did not significantly affect their coefficients of static and kinetic friction or their coefficients of rolling resistance and rolling friction. The above is due to considerable scatter of the analyzed traits, rather than inadequate selection of the evaluated dependencies, as illustrated by the example in Figure 2. For this reason, the search for more complex models of the analyzed relations is not justified. In a study of cereal grains, no correlations were observed between the physical attributes of seeds and their coefficients of static and kinetic friction

(KALINIEWICZ 2013b). An absence of correlations between frictional parameters and other physical attributes of seeds was also noted in studies investigating other types of seed material, including forest tree seeds (KALINIEWICZ, TROJANOWSKI 2011, KALINIEWICZ et al. 2011, KALINIEWICZ, POZNAŃSKI 2013).

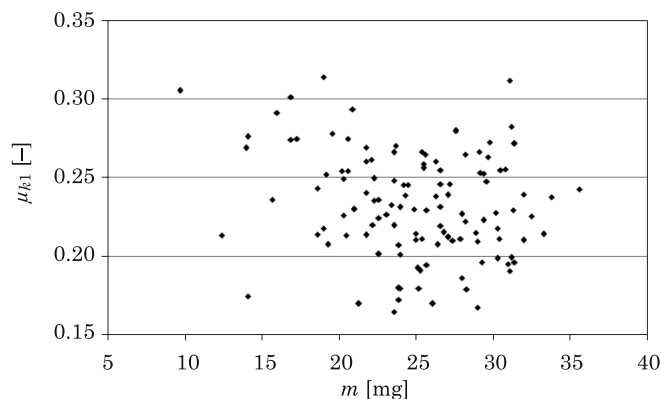


Fig. 2. Relationship between the weight of buckwheat seeds and their coefficient of kinetic friction on a steel friction surface

Significant correlations between the coefficients of static and kinetic friction of seeds moving on a steel surface were reported only for pea and faba beans. Similar correlations were noted in a study of cereal grains (KALINIEWICZ 2013b).

Summary

The analyzed seeds were characterized by a wide range of coefficients of static friction, from 0.187 (faba beans) to 0.426 (vetch) on a steel surface, and from 0.267 (faba beans) to 0.582 (buckwheat) on a rubber surface. Higher values of the analyzed coefficient on a rubber surface than on a steel surface can be explained by higher porosity and lower hardness of rubber.

Buckwheat seeds were the only seeds that moved on friction surfaces in sliding motion. Pea seeds were most susceptible to rolling. Approximately 62% of pea seeds on a steel surface and approximately 88% of pea seeds on a rubber surface initiated their motion by rolling. The values of the coefficient of rolling resistance were determined in the range of 0.148 (vetch seeds on steel) to 0.529 (pea seeds on rubber).

The coefficient of kinetic friction of seeds ranged from 0.140 (vetch) to 0.336 (pea) on a steel surface, and from 0.134 (pea) to 0.479 (buckwheat) on

a rubber surface. The average value of the coefficient of kinetic friction was by around 10% to 38% lower than the average value of the coefficient of static friction for seeds of a given species. The coefficient of rolling friction of seeds ranged from 0.29 to 1.34 mm on steel, and from 0.33 to 1.80 mm on rubber.

A statistical analysis revealed that the above frictional parameters were weakly correlated with the dimensions, weight, arithmetic and geometric mean diameter, aspect ratio and sphericity index of the examined seeds. Frictional properties were most significantly correlated with seed weight, although the strength of the observed correlations was relatively low.

Acknowledgements

I would like to thank Ms. Katarzyna Zalewska, MSc., Eng., and her doctoral advisor Mr. Stanisław Konopka, PhD., Eng., for providing me with access to the apparatus for measuring the external friction angle of seeds. I am also grateful to Ms. Aleksandra Poprawska for translating this paper into English.

References

- AFZALINIA S., ROBERGE M. 2007. *Physical and mechanical properties of selected forage materials*. Canadian Biosystems Engineering, 49: 2.23–2.27.
- ALTUNTAS E., DEMIRTOLA H. 2007. *Effect of moisture content on physical properties of some grain legume seeds*. New Zealand Journal of Crop and Horticultural Science, 35: 423–433.
- BAGHERPOUR H., MINAEI S., KHOSH TAGHAZA M.H. 2010. *Selected physico-mechanical properties of lentil seed*. International Agrophysics, 24: 81–84.
- BOAC J.M., CASADA M.E., MAGHIRANG R.G., HARNER III J.P. 2010. *Material and interaction properties of selected grains and oilseeds for modeling discrete particles*. Transactions of the ASABE, 53(4): 1201–1216.
- DARVISHI H. 2012. *Moisture-dependent physical and mechanical properties of white sesame seed*. American-Eurasian Journal of Agricultural & Environmental Sciences, 12(2): 198–203.
- DAVIES R.M., EL-OKENE A.M. 2009. *Moisture-dependent physical properties of soybeans*. International Agrophysics, 23: 299–303.
- FIROUZI S., ALIZADEH M.R., AMINPANAH H., VISHEKAEI M.N.S. 2012. *Some moisture-dependent physical properties of bean seed (Phaseolus vulgaris L.)*. Journal of Food, Agriculture & Environment, 10(3–4): 713–717.
- FRĄCZEK J. 1999. *Tarcie ziarnistych materiałów roślinnych*. Zeszyty Naukowe Akademii Rolniczej im. H. Kołłątaja w Krakowie, Rozprawy, 252.
- GHARIBZAHEDI S.M.T., MOUSAVI S.M., GSHAHDERIJANI M. 2011. *A survey on moisture-dependent physical properties of castor seed (Ricinus communis L.)*. Australian Journal of Crop Science, 5(1): 1–7.
- GRĘŃ J. 1984. *Statystyka matematyczna. Modele i zadania*. PWN, Warszawa.
- GROCHOWICZ J. 1994. *Maszyny do czyszczenia i sortowania nasion*. AR, Lublin.
- HORABIK J. 2001. *Charakterystyka właściwości fizycznych roślinnych materiałów sypkich istotnych w procesach składowania*. Acta Agrophysica, 54.
- IDOWU D.O., ABEGUNRIN T.P., OLA F.A., ADEDIRAN A.A., OLANIRAN J.A. 2012. *Measurement of some engineering properties of sandbox seeds (Hura crepitans)*. Agriculture and Biology Journal of North America, 3(8): 318–325.

- IZLI N., UNAL H., SINCİK M. 2009. *Physical and mechanical properties of rapeseed at different moisture content*. International Agrophysics, 23: 137–145.
- JOUKI M., KHAZAEI N. 2012. *Some physical properties of rice seed (Oriza sativa)*. Research Journal of Applied Sciences, Engineering and Technology, 4(13): 1846–1849.
- KABAS O., YILMAZ E., OZMERZI A., AKINCI I. 2007. *Some physical and nutritional properties of cowpea seed (Vigna simensis L.)*. Journal of Food Engineering, 79: 1405–1409.
- KALETA A., GÓRNICKI K. 2008. *Safe grain storage – the study of the issue*. Inżynieria Rolnicza, 1(99): 137–143 (article in Polish with an abstract in English).
- KALINIEWICZ Z. 2011. *Sito strunowe*. Zgłoszenie patentowe nr P.396745, 24.10.2011.
- KALINIEWICZ Z. 2013a. *String sieve: design concept and parameters*. Technical Sciences, 16(2): 119–129.
- KALINIEWICZ Z. 2013b. *Analysis of frictional properties of cereal seeds*. African Journal of Agricultural Research, 8(45): 5611–5621.
- KALINIEWICZ Z., GRABOWSKI A., LISZEWSKI A., FURA S. 2011. *Analysis of correlations between selected physical attributes of Scots pine seeds*. Technical Sciences, 14(1): 13–22.
- KALINIEWICZ Z., POZNAŃSKI A. 2013. *Variability and correlation of selected physical attributes of small-leaved lime (Tilia cordata Mill.) seeds*. Sylwan, 157(1): 39–46 (article in Polish with an abstract in English).
- KALINIEWICZ Z., TROJANOWSKI A. 2011. *Variability analysis and correlation of selected physical properties of black alder seeds*. Inżynieria Rolnicza, 8(133): 167–172 (article in Polish with an abstract in English).
- KALKAN F., KARA M. 2011. *Handling, frictional and technological properties of wheat as affected by moisture content and cultivar*. Powder Technology, 213: 116–122.
- KARA M., BASTABAN S., ÖZTÜRK I., KALKAN F., YILDIZ C. 2012. *Moisture-dependent frictional and aerodynamic properties of safflower seeds*. International Agrophysics, 26: 203–205.
- KARAJ S., MÜLLER J. 2010. *Determination of physical, mechanical and chemical properties of seeds and kernels of Jatropa curcas L.* Industrial Crops and Products, 32: 129–138.
- KIBAR H., ÖZTÜRK T. 2008. *Physical and mechanical properties of soybean*. International Agrophysics, 22: 239–244.
- KILIÇKAN A., ÜÇER N., YALÇIN I. 2010. *Moisture-dependent physical properties of black grape (Vitis vinifera L.) seed*. Scientific Research and Essays, 5(16): 2226–2233.
- KRAM B.B. 2006. *Research on the coefficient of external friction of corn grain in humidity function*. Inżynieria Rolnicza, 3(78): 175–182 (article in Polish with an abstract in English).
- KRAM B.B. 2008. *Investigation of the external friction coefficient and the angle of natural repose of cv. Bar and Radames lupine seeds*. Inżynieria Rolnicza, 4(102): 423–430 (article in Polish with an abstract in English).
- LAWROWSKI Z. 2008. *Tribologia. Tarcie, zużywanie i smarowanie*. Oficyna Wydawnicza Politechniki Wrocławskiej, Wrocław.
- ŁUKASZUK J., MOLENDĄ M., HORABIK J., WIĄCEK J. 2009. *Method of measurement of coefficient of friction between pairs of metallic and organic objects*. Acta Agrophysica, 13(2): 407–418 (article in Polish with an abstract in English).
- MOHSEENIN N.N. 1986. *Physical properties of plant and animal materials*. Gordon and Breach Science Public, New York.
- MOLENDĄ M., HORABIK J., GROCHOWICZ M., SZOT B. 1995. *Tarcie ziarna pszenicy*. Acta Agrophysica, 4. Instytut Agrofizyki im. Bohdana Dobrzańskiego, Lublin.
- NOSAL S. 2012. *Tribologia. Wprowadzenie do zagadnień tarcia, zużywania i smarowania*. Wydawnictwo Politechniki Poznańskiej, Poznań.
- RABIEJ M. 2012. *Statystyka z programem Statistica*. Helion, Gliwice.
- RAZAVI S.M.A., FARAHRMANDFAR R. 2008. *Effect of hulling and milling on the physical properties of rice grains*. International Agrophysics, 22: 353–359.
- RIYABI R., RAFIEE S., DALVAND M.J., KEYHANI A. 2011. *Some physical characteristics of pomegranate, seeds and arios*. Journal of Agricultural Technology, 7(6): 1523–1537.
- RUDZIŃSKI R. 2011. *Rules for storage and warehousing of goods of agricultural origin*. Zeszyty Naukowe Uniwersytetu Przyrodniczo-Humanistycznego w Siedlcach, Seria: Administracja i Zarządzanie, 88: 113–126 (article in Polish with an abstract in English).

- SHAROBEEM Y.F. 2007. *Apparent dynamic friction coefficients for grain crops*. Misr Journal of Agricultural Engineering, 24(3): 557–574.
- SHIESHAA R.A., KHOLIEF R., EL MESEERY A.A. 2007. *A study of some physical and mechanical properties of seed melon seed*. Misr Journal of Agricultural Engineering, 24(3): 575–592.
- SHOUGHY M.I., AMER M.I. 2006. *Physical and mechanical properties of faba bean seeds*. Misr Journal of Agricultural Engineering, 23(2): 434–447.
- SOLOGUBIK C.A., CAMPANONE L.A., PAGANO A.M., GELY M.C. 2013. *Effect of moisture content on some physical properties of barley*. Industrial Crops and Products, 43: 762–767.
- ŚLIPEK Z., KACZOROWSKI J., FRĄCZEK J. 1999. *Analiza teoretyczno-doświadczalna tarcia materiałów ziarnistych*. Ed. PTIR, Kraków.
- TAHERI-GARAVAND A., NASSIRI A., GHARIBZAHEDI S.M.T. 2012. *Physical and mechanical properties of hemp seed*. International Agrophysics, 26: 211–215.
- TARIGHI J., MAHMONDI A., RAD M.K. 2011. *Moisture-dependent engineering properties of sunflower (var. Armaviriski)*. Australian Journal of Agricultural Engineering, 2(2): 40–44.
- TASER O.F., ALTUNTAS E., OZGOZ E. 2005. *Physical properties of Hungarian and common vetch seeds*. Journal of Applied Sciences, 5(2): 323–326.
- YALÇIN Y. 2007. *Physical properties of cowpea (Vigna sinensis L.) seed*. Journal of Food Engineering, 79: 57–62.
- YALÇIN I., ÖZARSLAN C. 2004. *Physical properties of vetch seed*. Biosystems Engineering, 88(4): 507–512.
- YALÇIN I., ÖZARSLAN C., AKBAŞ T. 2007. *Physical properties of pea (Pisum sativum) seed*. Journal of Food Engineering, 79: 731–735.

SELECTED ASPECTS OF DESIGNING AND REALIZATION OF LOW ENERGY SINGLE-FAMILY HOUSES ACCORDING TO THE NF15 AND NF40 STANDARDS

*Barbara Maria Deja*¹, *Jan Tyburski*²

¹ Department of Building Engineering and Building Physics

² Department of Foreign Language Studies
University of Warmia and Mazury in Olsztyn

Received 9 October 2014; accepted 6 March 2015; available on line 12 March 2015.

Key words: design and realization of single-family houses, the NF40 and NF15 energy standards, low energy building, passive building.

Abstract

The article presents chosen aspects of designing and realization of low energy single-family houses fulfilling the requirements of the NF40 and NF15 standards as determined in the priority program of the National Fund for Environmental Protection and Water Management entitled „An improvement of energy effectiveness. Subsidies to low energy houses”. An analysis concerns the minimal technical requirements pertaining to the outside shape and internal structure of NF40 and NF15 buildings, in comparison with the building law recommendation on technical conditions to meet by buildings and their location. An attention was paid to chosen problems of fulfilling the requirements of the NF40 and NF15 standards and the need of applying modern structural and material solutions and to especially accurate realization.

Introduction

Because of the necessity of lowering energy consumption in the building sector, the EU ratified amendments to the Directive EPDB 2010/31/UE on 19 March 2010 concerning the energetic characteristic of buildings. An important postulate encompassed in this directive is an obligation of the Member States; governments to introduce financial and market incentives promoting construction of low energy buildings (Directive 2010/31/EU of the European Parliament and of the Council of 19 May 2010).

Correspondence: Barbara Maria Deja, Zakład Budownictwa Ogólnego i Fizyki Budowli, Uniwersytet Warmińsko-Mazurski w Olsztynie, ul. Heweliusza 4, 10-724 Olsztyn, phone: 48 609 902 069, e-mail: barbara.deja@uwm.edu.pl

One of the form of realization of this recommendation is the Poland-wide program of subsidies for a low energy building which was worked out by the National Fund for Environmental Protection and Water Management (NFOŚiGW) and introduced for the period of 2013–2018. This program, which is being realized with the public financial resources, is aimed at the investors who build or buy single-family houses or flats in multi-family dwellings, which meet the requirements of the two standards: the NF40 low energy one or the NF15 passive (ŻURAWSKI 2013).

The symbols of the NF40 and NF15 standards represent the annual demand for a usable energy for the heating and ventilation $EU_{c.o.}$ of respectively 40 and 15 kWh/(m² · year), calculated in accordance with the principles determined in the standard (PN EN ISO 13790: 2009) using the monthly or hourly method including the weather data published by the Ministry of Transport, Construction and Maritime Economy as well as the relevant standards encompassed in the list of the Polish Committee of Standardization.

For the requirements of the program, the Polish National Energy Conservation Agency (KAPE) has elaborated an expert appraisal pertaining to the principles of designing and realization of low energy houses in Poland. This elaboration became the basis for the Recommendations approved by the Board of NFOŚiGW, determining the mandatory requirements for reaching expected energetic standards of residential houses and the way of design verification and checking the reliability of the construction (*Domy Energooszczędne. Podręcznik dobrych praktyk* 2012).

Each building which is being realized in the framework of the program must obligatorily fulfill the technical requirements of the Recommendations. It was also foreseen that the practical application of the technical requirements will be a subject to periodical analysis and, if need be, the Recommendations will be amended.

1.5 year after the initiation of the program, in August 2014, the technical requirements concerning the building designing in the NF40 and NF15 energy standards were modified. The diversification of criteria based on the climatic zones in Poland was abandoned.

The modified minimal technical requirements for residential houses, being realized according to the NF40 or NF15 energy standards, are available at the internet page of NFOŚiGW (*Attachment No 3 to the priority program of NFOŚiGW* 2014).

The article analyses the current technical requirements concerning the structure of single-family houses, fulfilling the NF40 and NF15 energy standards and, on the basis of a review of professional literature as well as the results of our own papers, the most significant problems of the designing in accordance with these requirements were pinpointed.

The chosen minimal technical requirements for single-family houses being realized in the NF40 and NF15 standards

The minimal technical requirements for single-family houses in the NF40 low energy or NF15 passive standards were divided into five groups pertaining to:

- liminary requirement for usable energy for the purpose of heating and ventilation $EU_{c.o.}$,
- building structure,
- parameters of mechanical blow-in and blow-out ventilation systems with heat salvage,
- parameters of the heating systems and heating installation,
- parameters of the systems and installation for preparation of warm usable water.

In Table 1, the minimal technical requirements in the scope of construction timing to enhance thermal insulation capacity of the building envelope and to minimize the heat losses in single-family houses fulfilling the NF40 and NF15 energy standards were presented.

In the second column of Table 1, the technical requirements concerning the structure of traditionally designed single-family houses, i.e. according to the recommendations of the Technical Conditions which have been in force in Poland since 1 Jan. 2014 (Decree of the Minister of Transport, Construction and Maritime Economy from 5.July. 2013).

In Table 1, the requirements in the scope of the liminary linear values of thermal losses coefficients of other thermal bridges do not apply to concave corners of external walls and other geometrical bridges in the building envelope in the cases, when in the places of occurrence of these bridges the same material and constructional solutions were used as in the case of the components of the building envelope.

For the NF15 and NF40 standards the values of $\Psi \leq 0,15 \text{ W}/(\text{m} \cdot \text{K})$ are allowed for the thermal bridges, but only in the case of constructing a building on the ground (strip foundations, spot footings, floors on the ground etc.) and in the case of floors separating dwelling rooms from underground garages.

An analysis of the specified, selected minimal technical requirements shows that the buildings constructed according to the NF40 and NF15 energy standards are characterized by considerably lower (respectively ca. 2 and over 5 times smaller) values of the annual demand for the heating and ventilation $EU_{c.o.}$, in comparison to the values attained in a building designed according to the currently binding building law in Poland.

The attainment of such a low value of annual energy demand in low energy buildings requires to design the shape and structure of a building in the way to

Table 1
Chosen minimal technical requirements for single-family houses in the NF40 and NF15 standards and according to the Technical Conditions 2014 (WT 2014)

Energy standard of a building	WT 2014	NF 40	NF 15
Annual demand for a usable energy for the heating and ventilation $EU_{c.o.}$ [kWh/(m ² · year)]			
–	ca. 80.0	≤ 40.0	≤ 15.0
Limitary values of the thermal transmittance coefficient of the building envelope U_{max} [W/m ² · K]			
External walls	0.25	≤ 0.15	≤ 0.10
Roofs, flat roofs and ceilings under unheated attics or above passages	0.20	≤ 0.12	≤ 0.10
Ceilings over unheated cellars and enclosed under-floor spaces	0.25	≤ 0.20	≤ 0.12
Floors on the ground	0.30	≤ 0.20	≤ 0.12
Windows, balcony doors and transparent non-opening partitions	1.30	≤ 1.00	≤ 0.80
Roof windows	1.50	≤ 1.00	≤ 0.80
External and garage doors	1.70	≤ 1.30	≤ 0.80
Limitary values of linear coefficient of heat losses in thermal bridges Ψ [W/m · K]			
Balcony slabs	not determined	≤ 0.30	≤ 0.01
Other thermal bridges	not determined	≤ 0.10	≤ 0.01
Air-tightness of a building (mechanical ventilation) n_{50} [1/h]			
–	≤ 1.50	≤ 1.00	≤ 0.6

Source: Worked out by the authors: Attachment No 3 to the Priority Program of NFOŚiGW (2014) and Decree of the Minister of Transport, Construction and Maritime Economy (2013).

obtain an improvement of thermal insulation capacity of non-transparent partitions, windows and doors (a considerable limitation of value of thermal transfer coefficient) and to lower heat loss through thermal bridges and uptightness of external shells.

Thickness of insulation layers of the building envelope components in the single-family houses fulfilling the NF15 or NF40 standards

The improvement of the thermal insulation capacity of the components of the building envelope is obtained as a result of usage of load-bearing layer materials characterized by an appropriately high thermal resistance R and the adequate thickness of insulation layers made of the most energy effective materials.

Table 2
Specification of calculated thickness of external walls insulation layers required to fulfill the demands of the WT 2014, NF40 and NF15 energy standards

External walls				
Insulation layer		energy standard/limitary U -value		
Kind of thermal insulation material	thermal conductivity coefficient λ , W/mK	WT 2014 $U = 0.25$ W/m ² K	NF40 $U = 0.15$ W/m ² K	NF15 $U = 0.10$ W/m ² K
Load – bearing layer made of chequer brick (25 cm thick) $R = 0.55$ m ² K/W				
Required insulation thickness [cm]				
Mineral rockwool	0.037	12	22	34
Graphite styrofoam	0.032	11	19	30
Polyurethane boards	0.023	8	14	21
Load – bearing layer made of cellular concrete blocks YTONG ENERGO (24 cm thick) $R = 2.52$ m ² K/W				
Required insulation thickness [cm]				
Mineral rockwool	0.037	5	15	27
Graphite styrofoam	0.032	4	13	23
Polyurethane boards	0.023	3	9	17
Load – bearing layer made of clay blocks POROTHERM (38 cm thick) $R = 3.24$ m ² K/W				
Required insulation thickness [cm]				
Mineral rockwool	0.037	3	12	24
Graphite styrofoam	0.032	3	11	21
Polyurethane boards	0.023	2	6.5	15

Source: Elaboration of the authors.

Table 3
Specification of calculated thickness of roof insulation layers required to fulfill the demands of the WT 2014, NF40 and NF15 energy standards

Roofs				
10% share of wood in the heterogeneous layer with insulation was assumed for the calculation		energy standard/limitary U -value		
Kind of thermal insulation material	thermal conductivity coefficient λ , W/mK	WT 2014 $U = 0.20$ W/m ² K	NF40 $U = 0.12$ W/m ² K	NF15 $U = 0.10$ W/m ² K
Required insulation thickness [cm]				
Mineral rockwool	0.037	23	38	49
Graphite styrofoam	0.032	20	33	42
Polyurethane boards	0.023	14	23	30

Source: Elaboration of the authors.

In Tables 2, 3 and 4, the results of calculation of the thickness of insulation layers of chosen components of the building envelope (external walls, roofs and floors on the ground) for attaining the required U -value in single-family houses meeting the NF40 and NF15 energy standards are presented.

The calculations were performed according to the PN-EN ISO 6946:2008P standard „Building components and elements of a building. Thermal resistance and the coefficient of thermal transfer. The calculation method”.

Table 4
Specification of calculated thickness of floor-on-the ground insulation layer required to fulfill the demands of the WT 2014, NF40 and NF15 energy standards

Floor on the ground				
The thermal resistance of other layers was left out		energy standard/limitary U -value		
Kind of thermal insulation material	thermal conductivity coefficient λ , W/mK	WT 2014	NF40	NF15
		$U = 0.30 \text{ W/m}^2\text{K}$	$U = 0.20 \text{ W/m}^2 \text{ K}$	$U = 0.12 \text{ W/m}^2 \text{ K}$
Required insulation thickness [cm]				
Mineral rockwool	0.037	12	18	30
Graphite styrofoam	0.032	10	16	26
Polyurethane boards	0.023	8	11	19

Source: Elaboration of the authors.

From the analysis of the above presented results of the calculations issues that:

- the mandatory thickness of insulation layers for attaining the required U -values for non-transparent divisions are many fold bigger in the building fulfilling the NF40 or NF15 standards, as compared to the building designed according to the requirements of the Technical Conditions (WT 2014). For example, the insulation thickness from mineral rockwool of an external wall with a load – bearing layer from POROTHERM clay blocks of 38 cm thickness in the NF40 and NF15 buildings must be respectively 4 and 8 times bigger than in the buildings fulfilling the WT 2014 requirements;

- the thickness of an insulation layer mandatory to attain the needed U -values of non-transparent divisions depends on the thermal resistance of a material of the load – bearing layer. For example, in a NF15 building the change of the load – bearing layer material from chequer bricks 25 cm thick to cellular concrete block 24 cm thick or clay blocks 44 cm thick allows the reduction of the thickness of an insulation layer from mineral wool respectively by 20% and 56%;

– the mandatory thickness of an insulation layer for attaining the U -value of external walls depends on the thermal resistance of an insulation material. In the case of the YTONG ENERGO blocks (24 cm thick), the usage of polyurethane boards insulation, instead of mineral rockwool allows to reduce the thickness of an insulation layer by 37% (in a NF15 building).

Thermal bridges in the buildings fulfilling the NF40 or NF15 standards

To reduce the occurrence of thermal bridges in the low energy buildings, the following general principles are to apply:

– the insulation layer should surround the entire heated part of a building in a continuous and uninterrupted way, thus for example, the roof insulation layer should be connected with the external wall insulation over its entire length,

– everywhere, where it is possible, gaps, thickenings, or punctures in the insulation layer should be avoided,

– in the design of a building, sharp edges should be avoided, because they are difficult to insulate (e.g. it is especially difficult to maintain insulation continuity in the neighborhood of skylight windows),

– structural solutions should be used to promote insulation continuity, e.g. self-supporting balconies and foundation on the foundation slab.

In the calculations of the thermal transmittance coefficients of non-transparent partitions, corrections should be included for air gaps in the insulation layer, for mechanical fasteners going through an insulation layer, and for precipitation on a roof with inverted layers (Attachment No 3 to the priority NFOŚiGW program 2014).

The heat losses issuing from the occurrence of punctual thermal bridges should be limited by the choice of mechanical fasteners with pivots characterized by a low thermal conductivity coefficient and appropriate stoppers for closing openings in thermal insulations.

In the case of low single-family houses, not subject to strong wind, the mechanical fasteners can be abandoned and replaced by the gluing of the insulation to the wall. Gluing should be done in such a way which prevents air circulation between the insulation layer and the load-bearing wall, and also prevents slit occurrence between insulation sheets which could generate thermal losses. All sources of leakage in the insulation layer should be filled in with trims of insulation material used or with spray insulation (e.g. PUR caulk).

The minimal technical requirements for the NF40 or NF15 buildings necessitate that the assessment of the linear thermal transmittance coefficients resulting from heat transfer through thermal bridges should be done by conducting numerical calculations on the basis of the PN-EN ISO 10211:2008 standard. Thus it is unacceptable to apply simplified methods or to use the data taken from the thermal bridges catalogues.

The established in the technical conditions limitary values of linear thermal transmittance coefficients Ψ for the NF40 and NF15 buildings in the energy standard are very low (especially these for the NF15 standard buildings: $\Psi \leq 0.10$ W/mK). In the places, where there is a lack of continuous thermal insulation, the limitary values of linear thermal transmittance coefficients in thermal bridges Ψ are difficult to reach (GERYŁO et al. 2002). For example, in the common area of an external door with on-the-ground floor, as the thickness of the floor insulation increases, the value of the linear thermal transfer does not lower but it goes up (RYNKOWSKI 2014). It results from the fact that the thermal insulation of an on-the-ground floor with a thick layer of an insulator increases the temperature of basement soil, which augments the heat flow discharging in the contact place between the door and the floor. Hence the conclusion that the thickness of insulation layers of external partitions should be optimized, taking into account the required values of the linear thermal transmittance coefficients.

The fulfillment of the minimal energy NF40 or NF15 standards requirements pertaining to windows and external doors

In the minimal technical requirements for the buildings being constructed in the NF 40 and NF15 energy standards, the limitary values of the thermal transmittance coefficients for windows U_w were determined as not higher than 1.0 and 0.8 W/m² · K respectively. These are values, which are lower by 13.3% and 46.7% respectively than the limitary windows thermal transmittance coefficient determined in the Technical Conditions 2014 ($U_w = 1.5$ W/m² · K).

Yet it should be kept in mind that the values of the U_w -values depend on the thermal transmittance coefficients of the components of windows, i.e. of glassing (U_g), of frame (U_f) and of a distance frame (Ψ_g), and also on the windowpane share in the total surface of the window and the number of its divisions.

The designer should verify the producer's specifications for the calculation accurateness of the U_w -value, which should be done according to the PN-EN ISO 10077-1:2007 standard.

In the low energy buildings, a good solution is to use windows with a big glassing share (e.g. non-openable ones), which are characterized by the low U_w -values. While applying non-opening windows one should consider safety conditions, the necessity of airing a room in summer (in each room there should be at least one openable window) and the possibility of window cleaning from outside.

To attain low values of the linear coefficient of thermal losses through the rim of windows, the special construction of distance frames (so called warm distance frame) should be used as well as deeper setting of windowpanes in the window profile.

Windows in the buildings designed in the NF40 or NF15 energy standards should also fulfill the following additional requirements:

- so called warm assembly of windows should be used, i.e. in the layer of thermal insulation,

- the windows should be air-tight – the air infiltration coefficient for openable windows and balcony doors should amount not more than $n = 0.3 \text{ m}^3/(\text{m} \cdot \text{h} \cdot \text{daPa}^{2/3})$,

- because in NF40 and NF15 buildings, a gravity ventilation is not used but mechanical one with heat recovery, the windows cannot be equipped with diffusers,

- the connection of windows with the frame should be designed and realized in such a way as to attain their complete air-tightness.

An amount of solar gains has a very important significance for the energy efficiency of a building. Therefore glassed or transparent partitions of a low energy building should be characterized by a possibly high solar energy transmittance index, in the case of double- or triple-glazed panes $g \geq 0.60$ or $g \geq 0.50$ respectively (*Domy Energooszczędne. Podręcznik dobrych praktyk* 2012).

In view of the thermal comfort of the inhabitants, the protection of rooms against overheating is also important. Therefore in the windows and other glassed external partitions facing east, west and south, shading elements should be foreseen. The glassing shadowing solutions should not limit an access of solar radiation in winter. One of the simplest and at the same time most effective methods of glassing shadowing is planting a deciduous plant, which during the winter months stays leaf-less (it is possible to keep the needed natural lighting of the interior in winter).

The requirements concerning thermal insulation capacity of the entrance and garage doors in the NF40 and NF15 standard buildings are determined by the limitary values of thermal transmittance coefficients, $U_d = 1.3$ and $0.8 \text{ W/m}^2\text{K}$ respectively (Attachment No 3 to the priority NFOŚiGW 2014 program). These are values respectively 23.5% and 53% lower than the limitary U_d -values of entrance doors foreseen in the Technical Conditions 2014.

The requirements concerning the air-tightness of single-family houses fulfilling the NF40 or NF15 standards

In the minimal technical requirements for the buildings designed in the NF40 and NF15 energy standards, the limitary values of the coefficient expressing the number of air exchange between the external and internal environment (as a result of uptightness of a building at the pressure differences of 50 Pa) were determined at the level of $n_{50} \leq 1.0$ and $n_{50} \leq 0.6$ 1/h respectively. These are values of 1.5 or 2.5 times lower respectively than the limitary coefficient values of $n_{50} = 1.5$ 1/h determined in the Technical Conditions 2014.

The high level of building envelope's air-tightness in low energy buildings is aimed to eliminate thermal losses resulting from uncontrolled inflow of cold (and humid) air to the interior through gaps in the partitions. It should also protect against moistness and inter-layers condensation of steam, which might infiltrate to the leaky partition from the building interior (ZAKLIKOCKI 2014).

The attainment of the limitary values of the n_{50} coefficient in the buildings designed in the NF40 or NF15 standards requires a correct design of structural details and their painstaking realization.

The most important design recommendations concerning assuring the required air-tightness of a building are as follows:

- tight components of a building envelope should surround continuously and uninterruptedly the entire heated part,
- connections each components of the building envelope (e.g. at the meeting place of external wall and sloped roof) should be durable and air-tight, simple to make and inexpensive (these conditions are fulfilled by for example glued link with mechanical pressure),
 - each partition should have only one layer responsible for air-tightness,
 - determining the placement of the layer responsible for air-tightness, it should be considered that the diffusion resistance of a partition should be biggest from the inside and diminish towards outside,
 - an air-tight components of a building envelope, which usually at the same time fulfill the role of a vapour barrier, should be placed on the internal side of a partition, before the thermal insulation layer,
 - it is very important to make all kind of perforations through building casing air-tight, such as hook-ups, holes, electric sockets.

The air-tightness of NF40 and NF15 buildings should be checked at the construction stage, after the realization of all air-tight layers and the installations, which go through them by the means of air-tightness test (ŻURAWSKI 2013). The test is done according to the PN-EN 13829:2002 standard „The thermal properties of buildings. A valuation of air-tightness of buildings. The

method of pressure measurement with the aid of a ventilator” by usage of a blower door.

Summary and conclusions

The fulfillment of the criteria as determined by the minimal technical requirements for the buildings meeting the NF40 or NF15 energy standards in the scope of designing their outside shape and structure may be impeded by the following problems:

- the needed thickness of insulation layers of external partitions are very big (e.g. a roof in a NF15 building should be insulated with mineral wool at least 49 cm thick), which may cause problems of complicated assembly (e.g. in the case of a skylight window or a kneewall) and also may result in a considerable lowering of the usable height of an attic;

- attaining the required limitary values of the linear thermal transmittance coefficients may prove to be difficult in the case of thermal bridges in places lacking insulation continuity;

- the window carpentry designs in NF40 or NF 15 buildings should be especially conscientiously chosen because of the necessity of fulfilling a number of criteria: the proper geometry, air-tightness, proper U -value, as well as solar energy transmittance index;

- the postulate of the minimal technical requirements for the NF40 or NF15 standards to maintain a high level of air-tightness of a building is to be fulfilled only through the use of a high degree of accuracy achieved by specialist building teams.

On the basis of an analysis of the possibility of meeting the technical requirements for the buildings being constructed in the low energy or passive standards, the following practical conclusions may be stated:

- because of the very big thickness of traditional insulation in the building being realized in the NF40 or NF15 standards, other insulation materials should be applied, e.g. polyurethane boards, polyurethane foam or multilayer mats consisting of a few courses of bubble foil and highly reflexive screens, aerogels and nanogels (an aerogel board 17 cm thick allows to attain the wall's thermal transmittance coefficient $U = 0.010 \text{ W/m}^2\text{K}$), or vacuum insulation (a board 7 cm thick allows to attain the wall's thermal transmittance coefficient $U = 0.010 \text{ W/m}^2\text{K}$);

- elimination of the majority of thermal bridges (necessary for reduction of heat losses) is possible only in the case of careful design of the structural details of a building (e.g. self-supporting balconies, situating on the foundation slab made in a permanent shuttering made of insulating material of appropriate density and of proper compressive strength and dampness resistance);

– a good solution for improvement of thermal insulation capacity of partitions is a design of two-layer partitions. In the internal layer (protected by the external layer against atmospheric influences), an insulation continuity and maximal air-tightness as well as the removal of thermal bridges are being attained (BAĆ et al. 2014). Glazed fragments of external partition (e.g. Trombe's wall) enable to increase the share of solar gains in the energy balance of a building.

References

- BAĆ A., CEBRAT K., NOWAK Ł. 2014. *Podwójna przegroda w zrównoważonym domu blisko zeroenergetycznym*. Materiały Budowlane, 1: 22–23.
- GERYŁO R., KASPERKIEWICZ K., POGORZELSKI J.A. 2002. *Wpływ docieplenia ścian wielkopołytowych na możliwość ograniczenia mostków cieplnych*. Prace Instytutu Techniki Budowlanej, 1(121): 3–12.
- Domy Energooszczędne. Podręcznik dobrych praktyk*. 2012. On line: <http://www.nfosigw.gov.pl/srodko-krajowe/programy/doplata-do-kredytow-na-domy-energooszczedne/podrecznik-dobrych-praktyk/> (access: 14.12.2014).
- Directive 2010/31/EU of the European Parliament and of the Council of 19 May 2010 on the energy performance of buildings (Dz. U. UE L 153/13, 18 June 2010).
- PAWŁOWSKI K., LEWANDOWSKI Ł. 2013. *Kryteria oceny stolarki okiennej w aspekcie architektonicznym oraz energooszczędnym*. Izolacje, 3: 22–27.
- PN-EN ISO 13790:2009: *Energy performance of buildings – Calculation of energy use for space heating and cooling*.
- PN-EN ISO 6946:2008P: *Building components and building elements – Thermal resistance and thermal transmittance – Calculation method*.
- PN-EN ISO 10211:2008P: *Thermal Bridges In Building Construction – Heat Flows and Surface Temperatures – Detailed Calculations*.
- PN-EN ISO 10077-1:2007: *Thermal Performance Of Windows, Doors And Shutters – Calculation of Thermal Transmittance. Part 1: General*.
- PN-EN ISO 13788:2003-05E: *Hygrothermal performance of building components and building elements. Estimation of internal surface temperature to avoid critical surface humidity and assessment of the risk of interstitial condensation. Calculation methods*.
- Rozporządzenie ministra transportu, budownictwa i gospodarki morskiej z 5 lipca 2013 r. zmieniające rozporządzenie w sprawie warunków technicznych jakim powinny odpowiadać budynki i ich usytuowanie (DzU z 2013 r., nr 0, poz. 926).
- RYNKOWSKI P. 2014. *Problemy dostosowania mostków cieplnych do standardu NFOŚiGW*. Materiały Budowlane, 1: 34–43.
- ZAKLIKOCKI Ł. 2014. *Projekt domu jednorodzinnego w standardzie energetycznym NF15 z charakterystyką energetyczną budynku*. Praca inżynierska wykonana pod kierunkiem dr inż. Barbary M. Dei, UWM w Olsztynie.
- Załącznik nr 3 do programu priorytetowego NFOŚiGW. 2014. *Wytyczne określające podstawowe wymogi niezbędne do osiągnięcia oczekiwanych standardów energetycznych dla budynków mieszkalnych oraz sposób weryfikacji projektów i sprawdzenia wykonanych domów energooszczędnych*. On line: <http://www.nfosigw.gov.pl/srodko-krajowe/programy/doplata-do-kredytow-na-domy-energooszczedne/informacje-o-programie/> (access: 14.12.2014).
- ŻURAWSKI J. 2013. *Program dopłat do domów energooszczędnych*. Izolacje, 7/8(178): 18–21.

EXPERIMENTAL STUDY OF THERMAL PYROLYSIS OF TURKEY FEATHERS

*Dariusz Kardaś¹, Jacek Kluska¹, Jarosław Szuszkiewicz²,
Mateusz Szumowski¹*

¹ Institute of Fluid Flow Machinery
Polish Academy of Sciences in Gdańsk

² Department of Materials Technology and Engineering
University of Warmia and Mazury in Olsztyn

Received 9 October 2014; accepted 6 March 2015; available on line 12 March 2015.

Key words: thermal pyrolysis, turkey feathers, gaseous products, reactor.

Abstract

The analysis of chemical composition of turkey feathers reveals over 50% mass content of carbon. Unfortunately, the feathers contain also over 13% by weight of nitrogen and over 2.5% of sulfur. The significant presence of nitrogen and sulfur in turkey feathers indicates potential danger to the environment.

The experiments of thermal pyrolysis of turkey feathers were done from a perspective of energy production potential out of gaseous products.

The products of thermal pyrolysis were mainly gas and liquid. The calorific value of pyrolysed feathers is comparable with the one of hard carbon. It gets higher for higher temperatures. The calorific value of gaseous products of turkey feathers at 850°C was maximum and it equalled 16.7 MJ/Nm³.

Introduction

The consumption of poultry in Poland as well as Europe increases (*Annual Report of AVEC*. 2014). The trend is permanent and there are many reasons for that. The popularization of poultry is caused by its nutritive values, which help decrease cardiovascular diseases morbidity of human. The increase of poultry consumption was also caused by the occurrence of animal epidemic of cattle and pigs during the last two decades (eg. Creutzfeldt-Jakob disease).

In 2011 Poland was the fourth country in Europe regarding to poultry production which was 1300 thousand tons. Turkeys have a significant share in poultry production estimated at 340 thousand tons annually (BIEGAŃSKI 2014).

Correspondence: Dariusz Kardaś, Instytut Maszyn Przepływowych im. Roberta Szewalskiego Polskiej Akademii Nauk, ul. Fiszerka 14, 80-231 Gdańsk, phone: 48 58 6995166, e-mail: dariusz.kardas@imp.gda.pl

The production of such significant mass of poultry means a production of a considerably huge amount of feathers, which are mainly waste (KWIATKOWSKI, KRZYSZTOFORSKI et al. 2012). It is due to the characteristics of the production process of poultry including mechanical collection of the feathers. The annual production of poultry feathers in Poland comes to 70 thousand tons (KRAJCZYŃSKA 2010). In turn, the amount of acquired turkey feathers is estimated on a level of several dozen of thousand of tons. Such a big mass of feathers presents a serious problem considering logistic and waste disposal issues.

There have been several approaches to the utilization of feathers (BUMLA et al. 2012). Feathers have been used as a fertilizer. There have been attempts of production of fabric out of feathers (WOOL 2010). They might be added to plastic for auto parts (KOTA et. al. 2014). Owing to their strength they make plastic parts more durable.

Probably the most often applied method of feathers utilization is the thermal one. Considering the chemical composition of feathers it is probably the best solution to choose. There are two most popular methods of thermal utilization of feathers: gasification and pyrolysis (DUDYŃSKI et. al. 2012, KWIATKOWSKI et. al. 2012).

Commonly, gasification and pyrolysis are considered to be the same process, which is wrong (GIRODS et.al. 2009). Gasification requires reduced amount of oxygen to carry out the process. The amount of oxygen must be limited to ensure that combustion will not occur. Whereas pyrolysis is a thermal decomposing of organic material in absence of oxygen.

Pyrolysis may be processed as thermal or plasma one. Regular source of heat is sufficient to obtain processing temperatures up to 1000°C. Plasma pyrolysis requires far more heat which requires using a plasma source.

The main purpose of the experiment was to decompose turkey feathers. The crucial point of interest is the composition of gaseous products of thermal pyrolysis.

Material

Turkey feathers are not a homogenous material. There are several varieties of feathers which depends on what part of a turkey's body they cover. The examples of turkey feathers are shown in Figure 1a (powder down) and Figure 1b (quill). The shape and structure of the feathers have a significant influence on heat transfer in the reactor and this way they also influence the course of thermal pyrolysis. Turkey feathers acquired through mechanical harvesting are in fact deformed and torn and they create a shapeless mass (Fig. 1c).



Fig. 1. Examples of turkey feathers: *a* – powder down, *b* – quill, *c* – post-production feathers

In order to carry out the analysis of chemical composition, the turkey feathers were dried in an electric drier and then shredded.

The feathers were subject of the research and computation of their calorific value. In order to carry out that task, a KL-11 Mikado calorimeter was applied. The feathers obtained directly from the production line characterize with considerably high moisture contents ranging from 30% to 60%. For that reason the analysis was carried out using a dried sample. The investigation

showed that the Low Heating Value (LHV) of the dried feathers was equal to 20.37 MJ/kg and High Heating Value equalled 21.8 MJ/kg. These values are comparable with these of hard carbon.

The chemical composition analysis of turkey feathers (elementary composition) was done by Flash 2000 CHNS/O thermal analyzer and S8 Tiger X-ray fluorescence spectrometer with wavelength dispersion (WX-XRF). The results of the chemical analysis were presented in Table 1.

Table 1

Elementary composition of turkey feathers

Component elements of dry feathers	Amount [%]
C	51.5
H ₂	7.4
O ₂	23
N ₂	13.1
S	2.5
Cl	0.23

The analysis revealed the reasons of the high calorific value of feathers: C and H₂ comprise almost 59% of their composition. The analysis revealed presence of: N₂ (13.5%) and S (2.54%). The presence of these two elements in such a significant amount may lead to the synthesis of many toxic chemical compounds in high temperatures (especially in O₂ atmosphere).

Experimental

The purpose of the research was to utilize turkey feathers by thermal Pyrolysis and produce combustible gas (DUDYŃSKI 2012, BUAH 2007). The experiments have been carried out in the Institute of Fluid Flow Machinery of the Polish Academy of Sciences in Gdańsk. The reactor used in the experiment could reach maximum temperature of 900°C (BREBU et.al. 2011). The reactor is a welded construction, mainly made of heat-resistant steel. It is cylindrical shaped and its internal diameter equals 98 mm. It is equipped with an external induction heating system. There is a possibility to supply the reactor with inert gas (eg. Argon) by a dedicated additional stub pipe (provided).

The test – stand for the thermal pyrolysis of turkey feathers is presented in Figure 2. The reactor is equipped with a set of thermocouples which task is to control temperature inside of it. The pyrolytic gas leaving the reactor is put through the cooler and then directed to the scrubbers. The gaseous products are collected in tedlar bags.

The purpose of the experiment was to determine the influence of temperature in the reactor on concentration of the gaseous products of the pyrolysis. The sample of turkey feathers was placed into the reactor. After tight closing of the reactor, it was subjected to heating at the constant speed of 18°C/min. The amount of the gaseous products of the pyrolysis was investigated at the following temperatures: 400°C, 500°C, 700°C, 850°C and 900°C.

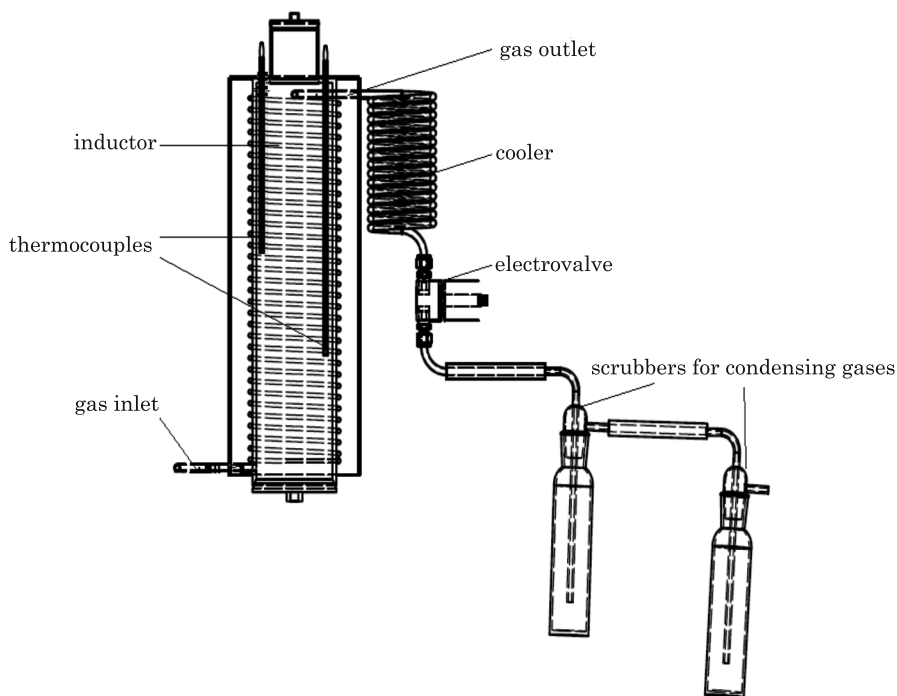


Fig. 2. Scheme of thermal pyrolysis test – stand of turkey feathers

The pyrolysis analysis showed formation of three states of the products: char, liquid and gas (KIM 2007). Their yields depended significantly on the process temperature. The amount of the formatted char reached value of 15.42% at 400°C and decreased to 1.86% at 900°C.

In the case of gaseous products of the pyrolysis their production increased when the temperature raised from 400°C to 700°C (Fig. 3). Further increase of the temperature caused decreasing of the gaseous products concentration: at 900°C the concentration dropped to 75%.

The amount of liquid products equalled 1.39 % for 400°C and monotonically increased up to 900°C, reaching finally the value of 23.14%.

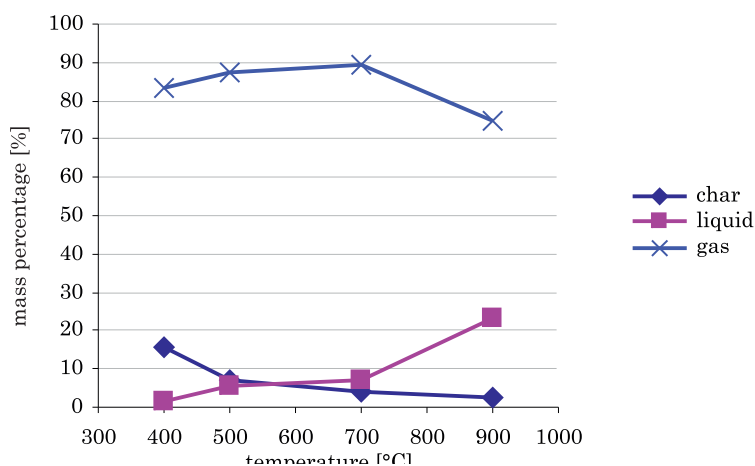


Fig. 3. Influence of pyrolysis temperature of turkey feathers on yields of products

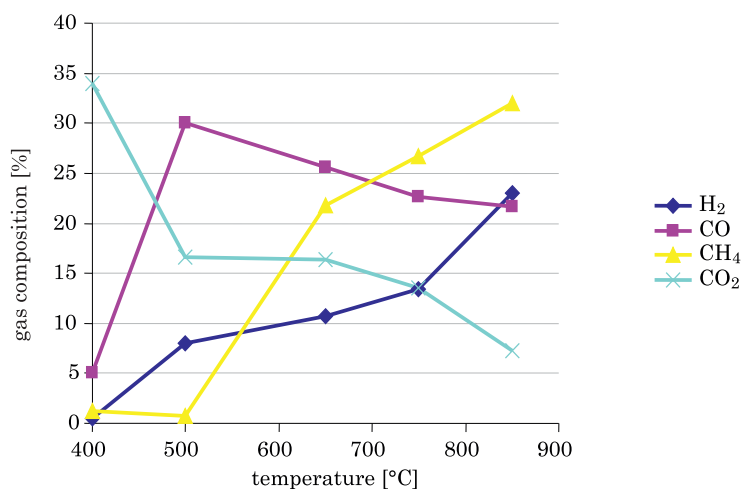


Fig. 4. Course of gas products concentration during thermal pyrolysis of feathers

The increase of temperature caused the increase of H₂ and CH₄ concentration. However, it decreased the CO₂ concentration (Fig. 4). On the other hand the CO concentration changed non monotonically: it increases with the increase of temperature up to 500°C and a further rise of the temperature causes a drop of it. The H₂ concentration for 400°C reaches the level of 0.5% and rises up to 23% at the temperature of 850°C. In the case of CH₄ analogically, its concentration rises from 1.2% to 32%. In the case of CO₂, for the same range of temperature, the concentration decreases from 35% down to 7%. The CO concentration reaches its maximum value at 500°C (30%).

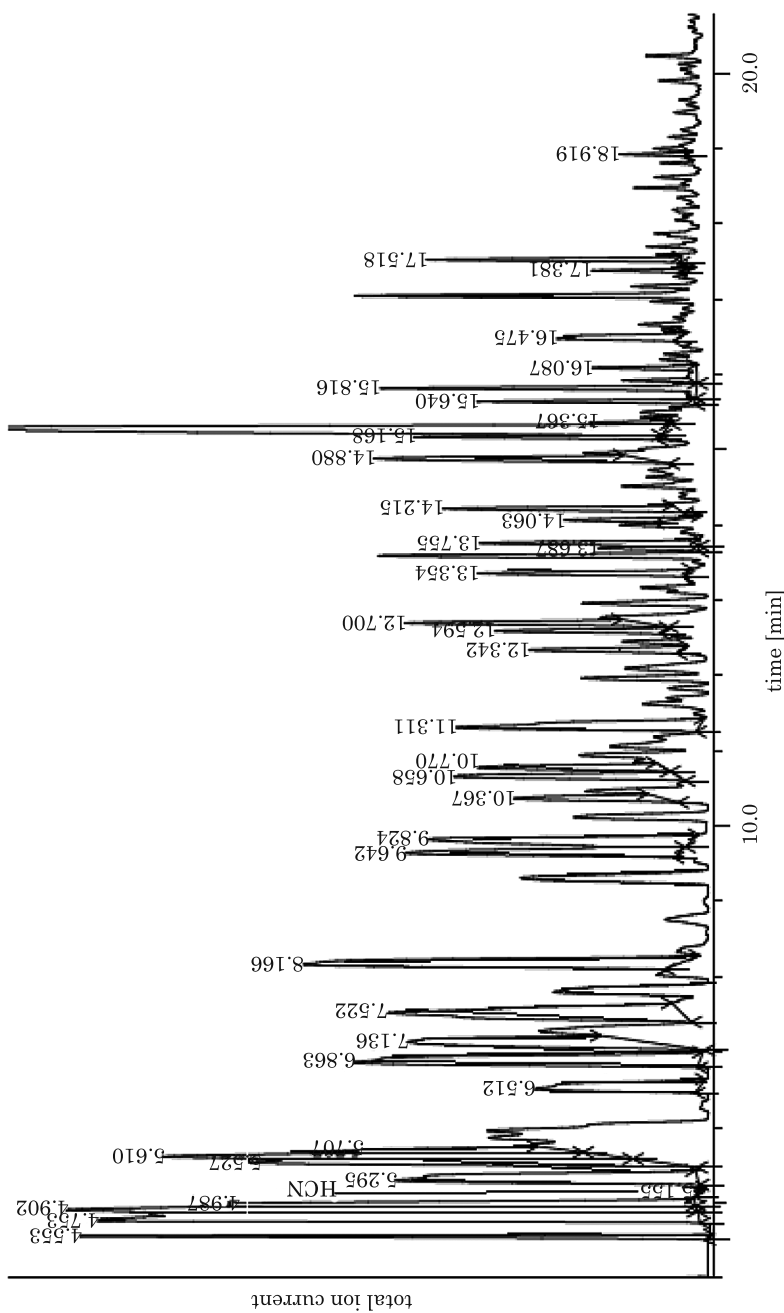


Fig. 5. Absorption spectrum showing presence of HCN in liquid products of thermal pyrolysis of feathers

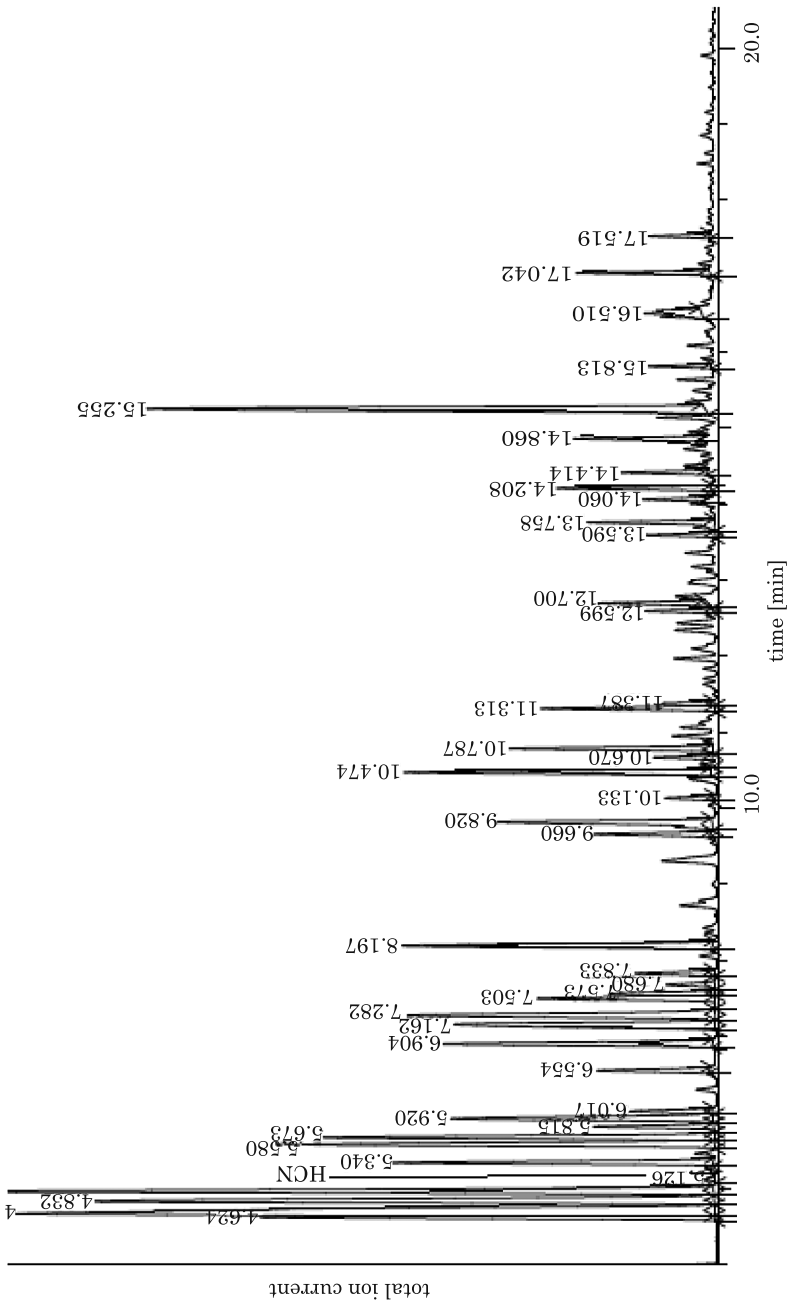


Fig. 6. Absorption spectrum showing presence of HCN in gaseous products of thermal pyrolysis of feathers

The calorific value of turkey feathers has been calculated on the basis of the gaseous products analysis. The minimum value of 1.2 MJ/Nm^3 was obtained at 400°C while the maximum value was obtained for 850°C and it was equal to 16.7 MJ/Nm^3 . The noticeable increase of the calorific value was caused by high content of CH_4 and H_2 at higher temperatures of the pyrolysis, at stable amount of carbon.

Sulfur contained in the feathers (Tab. 1) will be a potential threat if the gaseous products of the pyrolysis would be used as a fuel for energy generation. N_2 present in the turkey feathers (tab. 1) caused the synthesis of HCN in the pyrolysis products of the feathers (CZEPANKO 2010). That dangerous substance for the environment was identified in the liquid as well as in gaseous products of the pyrolysis (SENOZ 2011). The presence of the chromatographic bands of HCN is visible in the GC-MS spectra (Fig. 5, 6). The HCN band in the liquid products spectrum is visible at 5.092 min and in the gaseous products spectrum at 5.126 min.

Conclusions

The thermal pyrolysis research confirmed that this is the effective method of utilization of turkey feathers. In accordance with earlier assumptions, the pyrolysis products of turkey feathers have significant energy potential.

The gaseous products of the thermal pyrolysis might be used as energy source. Special precautions have to be taken with the gaseous products since they contain HCN. It is also present in the liquid products. Presence of S and N_2 will have negative consequences during production of energy in the process of combustion of the gaseous products, because it will lead to creation of SO_x and NO_x in the outgoing gas. To keep the process of combustion friendly and safe to the environment, an installation for energy generation should be equipped with an efficient and effective filtrating and cleaning system.

There was observed a monotonically increasing synthesis of the liquid products: 1.39% at 400°C to 23.14% at 900°C . The course of synthesis of char was monotonically decreasing: 15.42% at 400°C to 1.86% at 900°C . The course of synthesis of gaseous products was not monotonic. It was increasing from 83.19% at 400°C up to 89.54% at 700°C and then decreased to 75% at 900°C .

The raise of the process temperature caused the monotonic increase of the concentration of H_2 from 0.5% to 23%. Over 500°C the concentration of CH_4 was increasing. It reached 32% at 850°C . The concentration of CO_2 monotonically decreased from 35% to 7%. And finally, the concentration of CO is non monotonic: it increased from 5% at 400°C to 30% at 500°C and then decreased to 21% at 850°C .

There was observed the increase of the calorific value of the gaseous products of pyrolysis for higher process temperatures. The maximum calorific value was obtained for 850°C and it was 16.7 MJ/Nm³.

References

- Annual report of AVEC*. 2014. Association of Poultry Processors and Poultry Trade in the EU. On line: <http://www.avec-poultry.eu/system/files/archive/new-structure/avec/Annual-Report/2014/Version%20Finale.pdf>.
- BIEGAŃSKI M. 2014. *Produkcja indyków w 2013 roku*. Aktualności branżowe. Krajowa Rada Drobiarstwa. On line: <http://www.krd-ig.com.pl/produkcjaindykoww2013roku,756,11.html>.
- BISWAS M., MITTAL A., SRIKANTH G. 2009. *Composites: A vision for the future*. Technology Information, Forecasting and Assessment Council (TIFAC), Delhi. On line: http://www.tifac.org.in/index.php?option=com_content&view=article&id=539:composites-a-vision-for-the-future&catid=85:publications&Itemid=952.
- BREBU M., SPIRIDON I. 2011. *Thermal degradation of keratin waste*. Journal of Analytical and Applied Pyrolysis, 91: 288–295.
- BUAH W.K., CUNLIFFE A.M., WILLIAMS P.T. 2007. *Characterization of products from the pyrolysis of municipal solid waste*. Trans IChemE, Part B, Process Safety and Environmental Protection, 85: 450–457.
- BUMLA N.A., WANI S.A., RESHI I.M., ABASS M. 2012. *Processing and utilization of feathers*. Poultry Technology, 28 July.
- CZEPANKO V.B. 2010. *Assessment of air pollution when incinerating fermented waste with combustion gas components*. Chem. Process Eng., 31: 163–179.
- DUDYŃSKI M., KWIAKOWSKI K., BAJER K. 2012. *From feathers to syngas – Technologies and devices*. Waste Management, 32: 685–691.
- GIRODS P., DUFOUR A., ROGAUME Y., ROGAUME C., ZOUALIAN A. 2009. *Comparison of gasification and pyrolysis of thermal pre-treated wood board waste*. Journal of Analytical and Applied Pyrolysis, 85(1–2): 171–183.
- KIM S.S., AGBLEVOR F. 2007. *Pyrolysis characteristics and kinetics of chicken litter*. Waste Management, 27: 135–140.
- KOTA K., SHAIK S., KOTA K., KARLAPUD A. 2014. *Bioplastic from Chicken Feather Waste*. Int. J. Pharm. Sci. Rev. Res., 27(2): 373–375.
- KRAJCZYŃSKA E. 2010. *Polscy naukowcy wiedzą, jak mądrze wykorzystać nadmiar ptasich piór*. Nauka w Polsce. On line: <http://naukawpolsce.pap.pl/aktualnosci/news,369366,polscy-naukowcy-wiedza-jak-madrze-wykorzystac-nadmiar-ptasich-pior.html> (20 stycznia 2010).
- KWIAKOWSKI K., KRZYSZTOFORSKI J., BAJER K., DUDYŃSKI M. 2012. *Gasification of feathers for energy production – a case study*. Proceedings of 20th European Biomass Conference and Exhibition, Milan, p. 1858–1862.
- SENOZ E., WOOL R.P., MCCHALICHER C. 2012. *Physical and chemical changes in feather keratin during pyrolysis*. Polym. Degrad. Stab., 97: 297–307.
- WOOL R.P. 2010. *Microporous carbon-nitrogen fibers from keratin fibers by pyrolysis*. Journal of Applied Polymer Science, 118(3):1752–1765.

EXAMINING TECHNICAL SOLUTIONS FOR A PROTOTYPE OF A SOLAR-AIR COLLECTOR

*Jacek Leśny*¹, *Monika Panfil*², *Marek Urbaniak*¹,
*Roman Schefke*¹

¹ Department of Meteorology
University of Life Sciences in Poznań

² Department of Meteorology and Climatology
University of Warmia and Mazury in Olsztyn

Received 24 September 2014; accepted 20 January 2015; available on line 28 January 2015.

Key words: solar air collector, air humidity, evaporation potential.

Abstract

The research was conducted in the framework of the project known as „Coupon for innovations – support for the smallest companies”, endorsed by the Polish Agency for the Development of Business, and it had the following objectives: to assess the efficiency of the collector and reliability of the applied parameters such as the force of warm air blast, temperature increase depending on the intensity of solar radiation and the angle of the collector setup, influence of ambient temperature on the collector’s efficiency and heat loss, the quantity of relative humidity reduction correlative with the heating up of the flowing air. Collector in a standard installation position – on a vertical wall.

The assessed solar air collector was exposed to solar radiation and the following parameters were measured in the course of study: intensity of solar radiation falling on a vertical surface and on the collector’s surface (the collector was installed in vertical position, which is a standard installation method), temperature and velocity of air flowing into the collector as well as temperature and velocity of air flowing out of the device. The studies indicate that already at the radiation value of 100 W m^{-2} the collector worked efficiently and heated up the flowing air by about 5°C . This temperature increased together with radiation and reached the value of 20°C at the radiation of 800 W m^{-2} . The analysis of the collector’s efficiency showed that during its work (proper temperature and radiation) the efficiency remained at a satisfactory level from 42 to 46%.

Introduction

Solar collectors are nowadays a commonplace on roofs, walls or detached constructions, both in newly erected as in modernized buildings. The purchase of collectors is often subsidized by authorities on a local and national level. An

Correspondence: Jacek Leśny, Katedra Meteorologii, Uniwersytet Przyrodniczy w Poznaniu, ul. Piątkowska 94, 60-649 Poznań, e-mail: jlesny@up.poznan.pl

example of such policy is the program called: „Supporting dispersed renewable energy sources” implemented in Poland by National Fund for Environmental Protection and Water Management (NFOŚiGW). It involves mostly collectors which heat up a non-freezing fluid circulating in a closed circuit (e.g. a mixture of water with glycol etc.), which „transfers” the energy obtained from radiation to a battery in a form of a water tank. Such installation is relatively expensive and it requires electrical power supply in order to control and operate the circular pump. The device described and examined in this work is an air collector in which air is the directly heated factor. Additionally, this collector is equipped with photovoltaic cells propelling the fan which presses the heated air. Hence, it does not need an outer power supply but its work will be limited only to the time when it is exposed to direct sun radiation of an appropriate intensity. Thus, it can be stated that it uses radiation energy in a very simple way, similarly solar energy can be used by proper alignment of the building with the sun (CHWIEDUK, BOGDANSKA 2004). Knowledge on this subject is applied to build houses with low energy requirements, which is also described in literature (CHWIEDUK 2008, 2010).

Solar air collectors, which are additionally equipped with a photovoltaic module, have been produced only recently. Their advantages have been quite extensively described in the relevant literature and the research into improving them is still conducted (KHALEK et al. 2013, HUSSAIN et al. 2013, KRAMER, HELMERS 2013). Many studies have been also devoted to modeling the performance of such collectors (AMRIZA et al. 2013, KARIMA et al. 2014) and examining their efficiency (FENG et al. 2014, JIN-HEE et al. 2014, ABOLTINS et al. 2012, ABOLTINS, PALABINSKIS 2011), also some studies checked how they function in combination with water heating (FENG et al. 2013) and drying agricultural products (ABOLTINS, PALABINSKIS 2013).

Certainly collectors’ performance depends on the sole source of energy, namely the Sun, and the main solar element of the climate is insolation, i.e. the time in which direct solar radiation reaches the surface of the earth. Insolation depends mostly on the length of the day, cloudiness and transparency of the atmosphere. It has been estimated that in the area of Poland the biggest insolation occurs in the warm half-year (from March to September), with the maximum value in June in the north of the country (214 h), whereas the smallest insolation occurs in the cold half-year (the minimum value in December – 33 h), and the average insolation sum in Poland is 1526 hours (on average 4.1 h during the day) (KUCZMARSKI 1990, KUCZMARSKI, PASZYŃSKI 1981). The distribution of insolation in Poland is reflected in the values of total solar radiation which was estimated to be at the level of 3657 MJ m⁻² (BOGDAŃSKA, PODOGRODZKI 2000). Unfortunately big fluctuations on a yearly basis are a characteristic feature of the multiannual course of monthly values of

insolation in Poland, similarly as in the case of annual and seasonal values (PODSTAWCZYŃSKA 2007).

Aim topic of the investigation was examining technical solutions for a prototype of a solar-air collector and evaluation their work and efficiency.

Technical specifications of the collector prototype

The basic model of HC01S solar air collector consists of a welded frame from stainless steel which surrounds a plate made of multi-chamber polycarbonate, 5 mm thick, and a casing made from Al/Pe/Al composite plate (brand name Dibond TyhyssenKrupp). An absorber plate placed inside the casing is made of 1 mm thick aluminum sheet blackened on one side. The absorber is stiffened by a meander made from $23 \times 30 \times 2$ mm aluminum angles. Collector's dimensions are $118 \times 61 \times 7.5$ cm (height, width, thickness), weight: 9 kg. There is a 12 W/12 V photovoltaic panel, size 59×14 cm, built into the upper front part of the collector, in a separate chamber (for maintaining better thermal comfort, Fig. 1). In the upper rear part of the collector there is an inlet vent with a diameter of 100 mm (78.5 cm), in which a silent fan is installed – 92 mm, 3-18 V, max efficiency – $67,15 \text{ m}^3 \text{ h}^{-1}$, 2400 RPM. Nine vents with diameters of 1 cm (together 7.07 cm) in the lower part of the casing allow the



Fig. 1. Measurement station with the vertically installed solar air collector and sensors for measuring the radiation

air influx. Thermal isolation of the collector was made from chamber foil covered with metalized film. The collector is operated by an electronic regulatory device – two cranks – turn-on threshold and hysteresis, power supply of 12 V. In the lower part of the casing there is a switch which controls the collector' work in two modes:

1) first switch position (I) – operating mode as follows: battery > temperature sensor > regulator > operating mode selector – a fan in the outlet pipe stub (the so called winter mode i.e. heating);

2) second switch position (II) – operating mode as follows: battery > operating mode selector > fan (the so called summer mode – cooling the casing and sucking out the excess of hot air through a pipe connected to a room).

Standard installation of the collector on a vertical wall – according to the rules specified in the collector installation manual.

Method of research

The assessed solar air collector was exposed to solar radiation and the following parameters were measured for the research purposes: intensity of solar radiation, on a horizontal plane and on the collector's plane (the collector was installed vertically, which is a standard installation position), temperature and velocity of air influx as well as temperature and velocity of air flowing out of the collector.

Specialist meteorological equipment was used for the purpose of the study. These were two solar radiation sensors (Kipp & Zonen), CM11 and BF5 (Delta-T Devices) (Fig. 2), which measured total and dispersed radiation, two

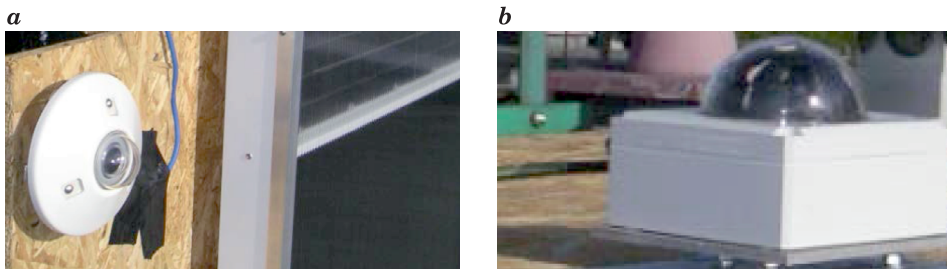


Fig. 2. Total radiation sensor – CN11 was placed vertically, according to the installed air solar collector (a) and total and dispersed radiation sensor – BF5 was placed horizontally (b)

sensors for measuring the temperature of incoming and outgoing air – E type thermocouples and IVL 10 channel speed and air temperature transducer (iBros Technic). All devices were connected to CR10X multichannel data logger with high measurement frequency (the recorder is built into the plug of the

USB interface, which ensures stable and effective monitoring of climate conditions, such as: temperature, insolation, air humidity etc.).

Then the software for data gathering and analysis was prepared. The above mentioned meteorological parameters of air flux were measured every second, whereas average values of measurements were recorded every minute.

Results and discussion

Measurements of short-wave radiation falling on a vertical surface (as in the surface of the collector) and on a horizontal surface, which is called, according to meteorological terms, total radiation, were conducted in October 2013 (during 15 days in total). However, for technical reasons, they were not conducted continuously, but with periodical breaks (the power supply conditions and the memory storage capacity of CR10X data logger). According to previous expectations, it was established that, due to the increasingly lower solar zenith, values of radiation falling on a vertical surface placed in the southern direction were much higher than the values of total radiation (Fig. 3).

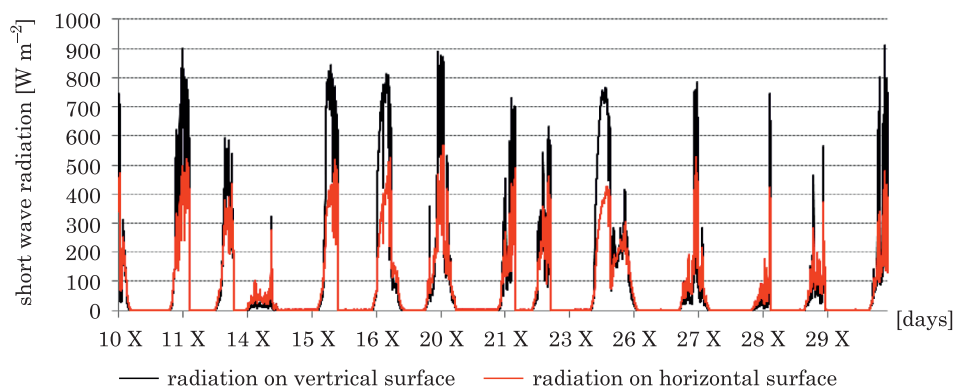


Fig. 3. Distribution of the measured short-wave radiation on a vertical surface (according to the collectors position) and a horizontal surface (total radiation), on 15 days selected in the period from 10 to 29 October 2013

The measured values as regards vertical surface sometimes exceeded 800 W m^{-2} , while the total radiation was merely of 500 W m^{-2} . It was very beneficial as regards the application of the assessed solar air collector. It can be definitely stated that the recommendation of the producer to install the collector on the southern wall in vertical position is very useful. In winter months (December-February) the differences between the radiation falling on

vertical and horizontal surfaces will be even bigger. Then, taking into consideration that the device is dedicated to work in the autumn-winter period, the suggested solution deserves a complete approval.

Next, the correlation between the flux velocity of the air measured at the outlet pipe stub of the solar air collector and the value of radiation falling on a vertical surface, similar to the position of the photovoltaic cells propelling the fan, was examined (Fig. 4). When analyzing the presented diagram one should bear in mind that the fan was turned on when the outside temperature exceeded 20°C, which meant that in some cases the fan was not turned on at all and the air flux could have been close to zero, although the radiation value did not go above 100 W m⁻². A similar situation occurred when the radiation was very low or close to zero, and the measured air fluxes, at the velocities of up to 0.2 m s⁻¹, resulted from a blowing wind. The collector is not tightly closed and when wind blows from a proper direction or when we are dealing with hydrostatic air circulation due to temperature differences, then air flux may occur even when the fan is inactive. Naturally, the higher radiation values the bigger air flux velocity (Fig. 4).

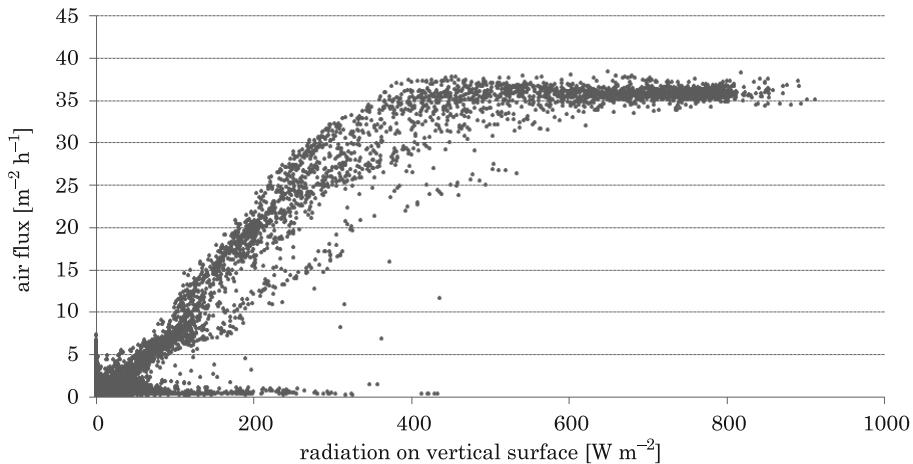


Fig. 4. Correlation between air flux at the outlet of the collector and the value of radiation falling on a vertical surface, compatible with the position of photovoltaic cells supply the fan

It is not a purely linear correlation and it is characterized by a relatively big dispersion, which is rather not surprising, just because of the fact that blowing wind may enhance or disturb the air flux. However, careful attention should be paid to the velocity of air flux in the outlet pipe, which increased to about 1.2 m s⁻¹ (ca. 36 m³ h⁻¹) reaching this value at the radiation of about 400 W m⁻².

Above this limit, despite the increase of the radiation value (up to 900 W m^{-2} during the measurements), the air flux did not become more intense. According to the producer the installed photovoltaic panel has the power of 12 W , which is several times bigger than the power of the fan, which leads to a conclusion that the above limitation does not stem from the lack of sufficient power. The producer claims the efficiency of the applied fan to be of about $60 \text{ m}^3 \text{ h}^{-1}$, however the air resistance in the collector significantly reduces the air flux, although the fan works at the highest engine power. The solution would be to lower the air flux resistance by enlarging inlet vents, changing – „making smoother” – the path of air flux or using simultaneously a second fan (possibly of a higher power).

Further, the distribution of air temperature was analyzed, after the air flowed through the solar air collector, depending on the solar radiation falling on a vertical surface (Fig. 5). In connection with the above, first the air temperature was measured at the inlet to the collector and then at the outlet. The measurements were conducted in the pipe about 5 cm from the fan (and not inside it), in order to determine temperature of the air flowing into the room „heated” by the collector reliably.

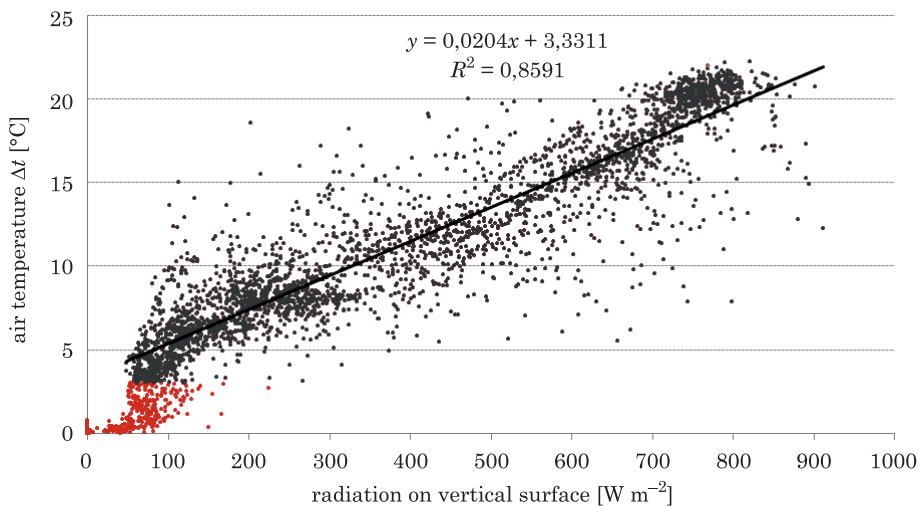


Fig. 5. Increase of air temperature after it flowed through the solar air collector in correlation with the radiation falling on a vertical surface (regression line was determined on the basis of only some minutes that had a temperature increase of more than 3.0°C)

Average minute values, when the temperature at the inlet and outlet of the collector was above 3.0°C , were marked in grey, which as the figure shows corresponded with the radiation of about 100 W m^{-2} and higher. Such radiation

range overlaps with the time when the fan was at work. These data were also used to determine the regression line. Red color marks the remaining points, while the figure does not take into consideration hours with zero radiation, when the collector certainly does not work.

The determined regression line (Fig. 5) was quite well correlated with the radiation values, determination coefficient (R^2) was 0.86. At the radiation values of 100 W m^{-2} the air flowing out of the collector reached the temperature of about 5.0°C , whereas at the radiation of 800 W m^{-2} these values were at the level of 20°C . It should be pointed out that, because of the schedule of the project known as „Coupon for innovation”, the research was conducted exclusively in October 2013, since the information about granting the funds for research and signing relevant contracts took place at the turn of September and October that year, and conducting the research, together with preparing the report was to have been finished until 31 October 2013. This research discipline resulted in its being conducted at the time when air temperature during the collector’s work was in the range from 10 to 20°C , and only on one measurement day the temperature dropped slightly below 10°C .

Relative air humidity is the quotient of the current steam pressure in the air and its maximum quantity in a given air temperature. It is one of the parameters of air humidity which reflects best the human perception of whether the air is dry or humid. If this value exceeds 80% then most people will say that the air is humid, while if it is below 50% they will declare it to be dry. This definition also leads to a conclusion that if the air having the humidity of about 70% is heated then its relative humidity falls, which means a simultaneous increase of its evaporation potential (drying potential).

Figure 6 illustrates the estimated change in relative humidity of the air flowing through the collector in correlation with the value of radiation falling on a vertical surface.

For the needs of the presented assessment it was adopted that relative humidity of the incoming air is 70% (average monthly humidity of the air in October at 12 UTC according to The Climate Atlas for Wielkopolska Region (FARAT 2004). Thus, it is clear that with the highest solar radiation values (800 W m^{-2}) humidity of the outgoing air will be only 20% and it will have high evaporation potential. This shows that at the lowest examined values for the collector’s work (100 W m^{-2}) the air at the outlet vent will have relative humidity of about 50%, which means that its evaporation potential is still relatively high. Summing up, the solar air collector should be quite efficient as a device for air heating and improving air drying potential.

On 25, 27 and 29 October 2013 there were changeable atmospheric conditions, but it was quite sunny and on each of these days the collector worked for several hours. Using the conducted measurements the amount

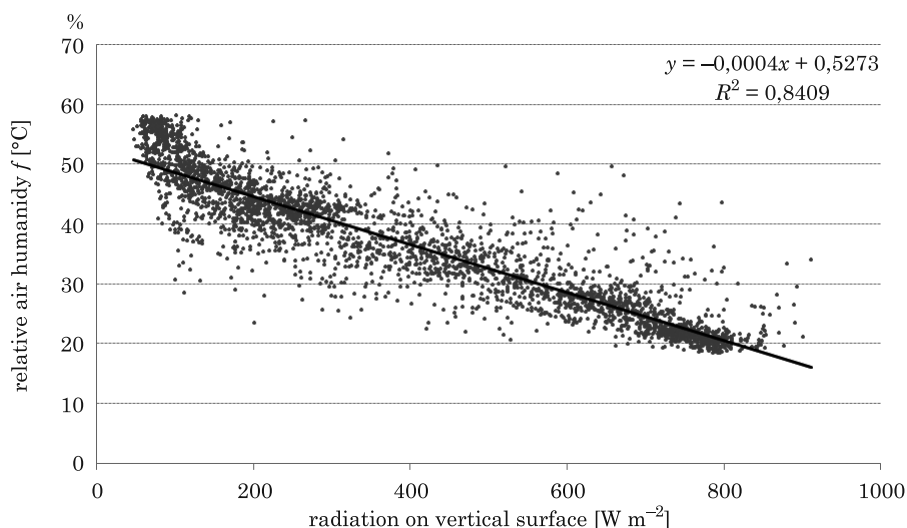


Fig. 6. Relative air humidity after flowing through the solar air collector in correlation with the radiation falling on the vertical surface, assuming that relative humidity of the air flowing into the collector is of 70%

of energy falling on the solar air collector was calculated, particularly on its part which serves for air heating. Only the time when the collector worked efficiently was taken into consideration, i.e. when its controller turned on the fan because temperature inside the collector exceeded 20°C and when simultaneously the radiation was strong enough to increase air flux through the collector to over 0.1 m s⁻¹. It turned out that on these days the collector's surface received cumulatively about 2580, 2700 and 3565 KJ respectively, whereas the air was heated to such an extent that the energy which transferred to the room had the values of 1180, 1140 and 1510 KJ respectively, and this in turn meant that the collector's efficiency at work was 46%, 42% and 42% respectively, a little more efficiency was obtained by ABOLTINS et al. (2012) and ABOLTINS and PALABINSKIS (2011). Thereby, the energy obtained on each of those days could serve as latent heat (of evaporation) to evaporate about 0.5 kg of water. It is necessary to mention that on those days from 50 to 100 m³ of air flowed through the collector and it ventilated the room on whose wall the collector was installed.

Summary and conclusions

1. The producer's recommendation to install the collector in vertical position on the southern wall of a building and adjusting it to work in this way is fully justified, because the measured values of radiation falling on a vertical surface sometimes exceed 800 W m^{-2} , while total radiation (on a vertical surface) reaches merely 500 W m^{-2} .

2. The resistance of air flux in the collector should be lowered by enlarging the inlet vents, changing – „smoothing” the way of air flux or using a second fan simultaneously (possibly of bigger power); because at the radiation of above 400 W m^{-2} , despite the fact that the fan's engine works at its highest efficiency, the air flux remains at the constant level of about $37 \text{ m}^3 \text{ h}^{-1}$ and does not reach the nominal efficiency value, i.e. $60 \text{ m}^3 \text{ h}^{-1}$.

3. Using such solutions as the cover from multi-chamber polycarbonate, black surface with slats absorbing solar radiation and chamber foil isolation covered with metalized film seem good ideas in terms of construction, since the studies indicate that already at the radiation value of 100 W m^{-2} the collector worked efficiently and heated up the flowing air by about 5°C . This temperature increased together with radiation and reached the value of 20°C at the radiation of 800 W m^{-2} .

4. On the basis of the conducted measurements it should be concluded that the solar air collector should efficiently perform its function as a device which heats up air and increases its drying potential because, assuming that the average relative humidity of the air flowing into the collector is 70%, at the highest radiation values the air flowing out of the collector will have only 20% humidity and high evaporation potential, and at the lowest values under consideration for the collector's work (100 W m^{-2}), it will have relative humidity of 50%, which means that its evaporation potential is still relatively high.

5. Despite high air flux resistance mentioned in point 2 the analysis of the collector's efficiency showed that during its work (proper temperature and radiation) the efficiency remained at a satisfactory level from 42 to 46%, which allowed obtaining from 1000 to 1500 KJ of energy in this time.

6. The schedule of the project imposed an imperative that the research be conducted when air temperature during the collector's operation was in the range from $+10$ to $+20^\circ\text{C}$, and only during one day of the measurements the temperature dropped slightly below $+10^\circ\text{C}$.

References

- ABOLTINS A., PALABINSKIS J. 2013. *New types of air heating solar collectors and their use in drying agricultural products*. *Agronomy Research*, 11(2): 267–274.
- ABOLTINS A., PALABINSKIS J. 2011. *Investigations of heating process and absorber materials in air heating collector*. *World Renewable Energy Congress 2011 – Sweden, Solar Thermal Applications (STH)*, p. 3991–3998.
- ABOLTINS A., RUSKIS G., PALABINSKIS J. 2012. *Air heated solar collectors and their applicability*. *Renewable Energy and Energy Efficiency, Solar energy applications and energy efficiency technologies in buildings*, Vienna, p. 212–217.
- AMORI K.E., ADIL ABD-ALRAHEEM M. 2014. *Field study of various air based photovoltaic/thermal hybrid solar collectors*. *Renewable Energy*, 63: 402–414.
- AMRIZAL N., CHEMISANA D., ROSELL J.I. 2013. *Hybrid photovoltaic-thermal solar collectors dynamic modeling*. *Applied Energy*, 101: 797–807.
- BOGDAŃSKA B., PODOGRODZKI J. 2000. *The variability of the total solar radiation on Polish territory in the period 1961–1995*. *Materiały Badawcze IMGW, Warszawa, Meteorologia*, 30: 43.
- CHWIEDUK D. 2008. *Some aspects of modeling the energy balance of a room in regard to the impact of solar energy*. *Solar Energy*, 82(10): 870–884.
- CHWIEDUK D. 2010. *Solar Energy Use for Thermal Application*. *Polish J. of Environ. Stud.*, 19(3): 473–477.
- CHWIEDUK D., BOGDAŃSKA B. 2004. *Some recommendations for inclinations and orientations of building elements under solar radiation in Polish conditions*. *Renewable Energy Journal*, 29: 1569.
- FARAT R. 2004. *Climate Atlas of the Wielkopolska Region*. Wydawnictwo IMGW, Warszawa.
- HUSSAIN F., OTHMAN M.Y.H., SOPIAN K., YATIM B., RUSLAN H., OTHMAN H. 2013. *Design development and performance evaluation of photovoltaic/thermal (PV/T) air base solar collector*. *Renewable and Sustainable Energy Reviews*, 25: 431–441.
- JIN-HEE K., SE-HYEON P., JUN-TAE K. 2014. *Experimental Performance of a Photovoltaic-thermal Air Collector*. *Energy Procedia*, 48: 888–894.
- KRAMER K., HELMERS H. 2013. *The interaction of standards and innovation: Hybrid photovoltaic-thermal collectors*. *Solar Energy*, 98(C): 434–439.
- KUCZMARSKI M. 1990. *Polish sunshine duration and its suitability for heliotherapy*. *Dokumentacja Geograficzna IGiZP PAN*, 4: 67.
- KUCZMARSKI M., PASZYŃSKI J. 1981. *Daily and seasonal variability sunshine duration in Poland*. *Przegląd Geograficzny*, 4: 779–791.
- PODSTAWCZYŃSKA A. 2007. *Characteristics of climate solar in Łódź*. *Acta Universitatis Lodziensis, Folia Geographica Physica*, 7: 220.
- SHAN F., CAO L., FANG G. 2013. *Dynamic performances modeling of a photovoltaic-thermal collector with water heating in buildings*. *Energy and Buildings*, 66: 485–494.
- SHAN F., TANG F., CAO L., FANG G. 2014. *Performance evaluations and applications of photovoltaic-thermal collectors and systems*. *Renewable and Sustainable Energy Reviews*, 33: 467–483.
- TOUAFEK K., HADDADI M., MALEK A. 2013. *Design and modeling of a photovoltaic thermal collector for domestic air heating and electricity production*. *Energy and Buildings*, 59: 21–28.

USE OF LIDAR DATA AND SELECTED ALGORITHMS FOR DETERMINING THE FLOW LINES

Zofia Szczepaniak-Koltun

Faculty of Civil Engineering, Environmental and Geodetic Sciences
Koszalin University of Technology

Received 19 October 2014; accepted 9 February 2015; available on line 18 February 2015.

Key words: Airborne Laser Scanning, flow lines, digital terrain model, algorithms D8 and MFD.

Abstract

This elaboration shows how to use Height Data by using airborne laser scanning (ALS) to delineation of flow lines which let to evaluation of water's flow on terrain.

Maps, which show flow lines, were generated by using GIS software and tools on testing areas. To achieve this goal were used methods of a single flow direction and multiple flow direction. Created maps which show directions of runoff, generated based on the DTM, were subjected to analysis. On the basis of these maps were evaluated the accuracy of determination of the flow direction on the testing areas by using individual algorithms.

Studies determining directions of runoff can and do have large application. They will serve the author as initium to create a network of watercourses needed to convert 3D image. This model of the network 3D will be an attempt to create a component BDOT10k in the form of three-dimensional.

Introduction

Quickly, easily, precisely – these terms can be safely attributed to the method of extraction of Height Data from airborne laser scanning (LIDAR). From these data we obtain accurate numerical models of terrain, which are use to execution of authentic spatial analysis in many diverse areas. Undoubtedly hydrology is the science that is closely associated with the lay of the land, and for which the DTM plays an important role in hydrological modeling. An important issue seems to be how the best delineation of flow lines because of the mutual relation between flowing water and form of land's surface. Distinction of runoff paths allows the determination of further phenomena necessary during modeling series of hydrological processes (e.g. accumulation of water

runoff, Soil Moisture Index, the ability of material's transformation – including pollution, determination of catchment's boundaries and many others). Assuming that the digital elevation model acquired from laser scanning is a precise sourcing material, it becomes reasonable to compare the most commonly used algorithms used for the extraction of the drain line.

Material and Methods

The source data

As the source data for delineation of flow lines were used elevation data from airborne laser scanning (LIDAR) collected within the ISOK (pol. Informatyczny System Osłony Kraju). This is the system of the country's protection against extreme hazards especially against flood. It is a project in Poland which aims to help improve the effectiveness of flood risk management. These data are available at National Geodetic and Cartographic Resource. The data in raster format was used for the extraction of flow lines by using SAGA GIS software.

Research area

For selection of the study area were used the following criteria:

- diverse in terms of hypsometry;
- diverse in terms of changes in water relations (both natural area and the changes in water management);
- forest area and an area with visible valleys on orthophotomap.

Due to these assumptions were chosen two test areas being part of a map M-33-44-C-a-2-2 (close to Jagniątków, the Karkonosze Foothills) and N-33-69-B-c-1-3 (close to Kłos, the north-eastern part of the Chełmska Hill).

Choice of the right algorithm

There are many algorithms allowing to determinate the water flow directions by using a raster DTM model. The essence of such modeling is to use the law of universal gravitation (gravity), which shows that water's flow go down the slope, from cells being situated higher into lower (URBAŃSKI 2011). There are three kinds of methods to create flow pathways, defined by different algorithms: single flow direction, multiple flow direction and „stream tube”

from one central cell (WILSON, GALLANT 2000). Undermentioned algorithms can be used to determine flow pathways:

Algorithm – Deterministic 8 (O'CALLAGHAN, MARK 1984). This algorithm is using for delineation of flow lines by calculating the difference in height between analysed raster cell and other, which surround her. Flow take place only to the one cell, for which obtained the highest value of the gradient (Fig. 1), hence this method is referred as single flow direction method (WOLOCK, MCCABE 1995).

Calculation of runoff takes place according to the following formula (1):

$$S_{D8} = \max_{i=1,8} \frac{z_9 - z_i}{h\phi(i)} \quad (1)$$

where:

z – the number of surrounding cell

h – resolution of GRID model

$h(\phi)$ – distance between the centres of cells, = 1 placed in the cardinal directions (north, east, south, west); the square root of 2 for others.

Algorithm Rho8 – Random eight-neighbour (random eight-node).

Rho8 algorithm is a modification of the classical stochastic-deterministic algorithm D8. It also marks single flow direction, however, defining the gradient is done by introducing the so-called random factor (hence the name of the method – a random eight-node), which makes that results are not reproducible. It is done in order to avoid long, parallel flow paths generated by using D8 algorithm (FAIRFIELD, LEYMARIE 1991).

Algorithms FD8 and FRho8. Algorithms FD8 and FRho8 are recognized in literature as Multiple Flow Direction – **MFD** (QUINN et al. 1991). They are a modification of D8 and Rho8 algorithms. As the name suggests, flow takes place in many directions, whereby this method has application to the determination of divergent flow. Part of surface runoff flowing out to the neighboring cell is transmitted based on calculation by the following formula (2):

$$P_i = \frac{\max(0, s_i^\alpha)}{\sum_{i=1}^8 (\max(0, s_i^\alpha))} \quad (2)$$

where:

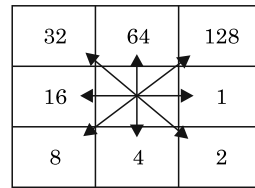
s_i – the size of the slope between the central node cells and neighboring cells

α – constant positive (recommended value $\alpha = 1.1$).

a

80	64	49	56	53
72	53	47	38	48
58	51	46	32	46
61	50	49	46	24
64	52	51	50	58

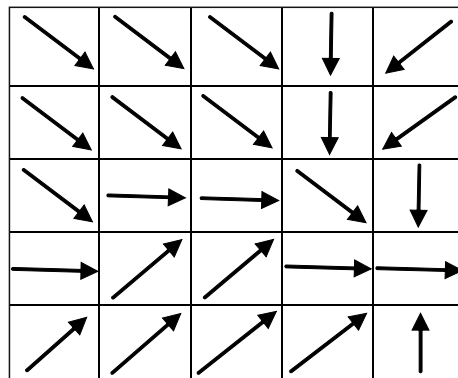
b



c

2	2	2	4	8
2	2	2	4	8
2	1	1	2	4
1	128	128	1	1
128	128	128	128	64

d



e

0	0	0	0	0
0	1	1	3	0
0	1	8	18	0
0	3	1	1	24
0	0	0	0	0

f

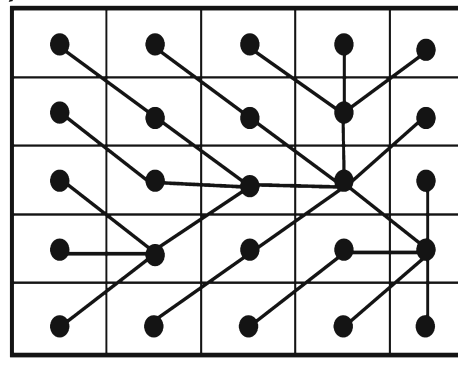


Fig. 1. Stages of determining runoff water with using the D8 method: *a* – DTM map, *b* – coding direction of flow using D8 method, *c* – map of the flow’s direction, *d* – the direction of runoff on the map, *e* – map of runoff’s accumulation, *f* – flow lines

Source: URBAŃSKI (2011).

Algorithm D_{∞} – Deterministic Infinity (TARBOTON 1997). The calculative method is based on the determination of runoff into two of the eight surrounding cells. Gradients of the biggest downslope is obtaining as a result of calculations made between the centre of the analysed cell and the centre of neighboring cells, which are connected with the eight triangles (Fig. 2).

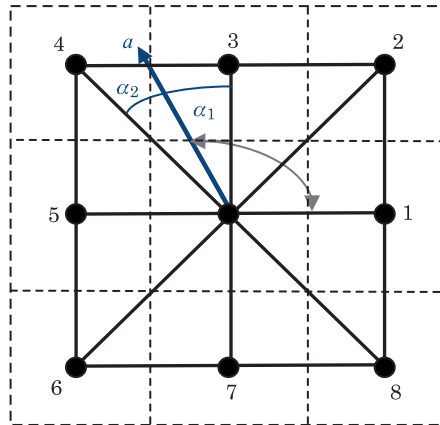


Fig. 2. Direction of runoff in the D_{∞} method: a – runoff direction, α_1 , α_2 – angles which determine the flow direction

Source: TARBOTON (1997).

Algorithm MD_{∞} – Triangular Multiple Flow Direction. It is a combination of MFD and D8 methods. Centres of cells are connected by triangles and algorithm proposed by Quinn is using for calculations.

Algorithm KRA – Kinematic Routing Algorithm. To determine the flow direction are used particular rastra cell, which are represented by plane fitted into corner points of the cell. Height of cells are determined by interpolation of height of neighboring centre cells, in addition flow direction is defined as the angle in the range from 0 to 2π (LEA 1992). Dispersion of flow does not occur in this method and the direction is determined in constant way.

Algorithm DEMON – Digital Elevation Model Networks (COSTA-CABRAL, BURGESS 1994). The direction of flow takes place in accordance with the terrain's drop to edge of DTM or to bottom of depression. It is directed whole to cell located below (when a specific direction of flow is a multiple of 90 degrees), or flow is split between two cells.

Algorithm BRM – Braunschweiger relief model. The direction of flow is maximum limited to three neighboring cells, to avoid excessive flow's dispersion (CONRAD 1998, PARK et al. 2009).

From presented above algorithms, to determine flow lines on the selected area, used two the most commonly used. These algorithms are D8 and MDF.

Method of determining flow lines

To elaboration was used a model of the terrain, with a regular grid with a mesh aperture of 1 meter, for which the average height error is in the range to 0.2 m. This model is available at the National Geodetic and Cartographic Resource. It was obtained from airborne laser scanning (ALS parameters are shown in Table 1) and interpolated on the base on points clouds for which the scan density on analyzed areas was 4pts/m² (the data saved in accordance with the standard 1.2 published in 2008 by the ASPRS – American Society for Photogrammetry and Remote Sensing).

Table 1

Basic Parameters ALS within ISOK

Parameters	Standard I: Non-urban areas
Transverse angle of scanning:	≤ + 25°
Density of points cloud:	≥ 4 points/m ²
Side overlap	≥ 20%
Height accuracy (mean error) of laser points	mh ≤ 0.15 m
Registration of intensity of reflected signals	yes
Conditions of photographic registration	medium format camera with color CCD with resolution greater than 30 M pixels
Flying height	helicopter 200–300 m areoplane 500–1000 m (max 6000 m)

Afterwards artificial artefacts were removed from DTM – „false sinks” – a collection of one or more cells, which from all sides are surrounded by other cells of bigger height value (URBAŃSKI 2011). Prepared in this way DTM was used to realise maps of surface flow. Extraction of flow lines occurred by using selected algorithms implemented in Saga GIS software. At the same time were assessed threshold values in order to determine of channel initiation threshold (Fig. 3). Received in the form of a vectorial network of flow lines were smoothed in order to obtain a better visualization.

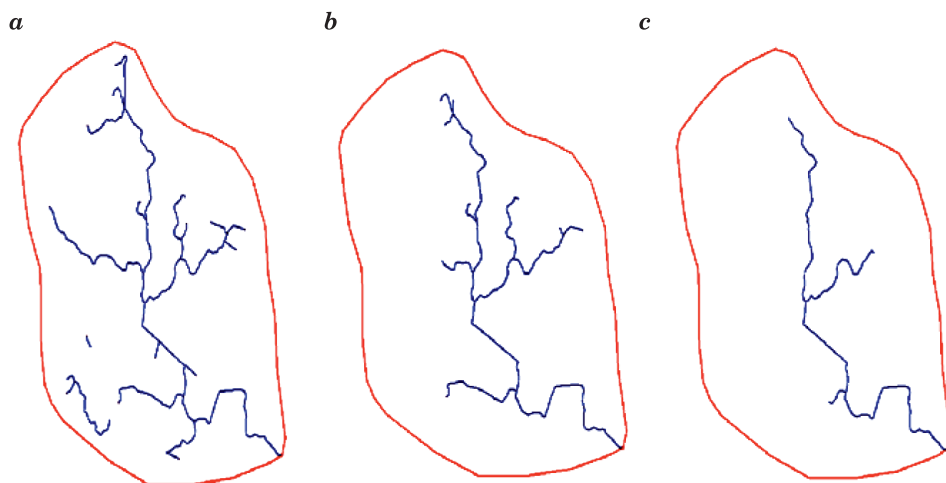


Fig. 3. The impact of the threshold value to determine density of the flow lines network: *a* – big, *b* – average, *c* – small

Results and Discussion

Comparison of algorithms D8 and MFD

Both applied algorithms gave similar results in determination of flow on the area of distinct valleys. On the analysed areas, marked out flow lines coincide almost the entire length (Fig. 4*a, b*) and the shape and course of the line is consistent with the land form.

Marked differences are visible when using both methods, in areas where hillside in big distances is rising in the same direction. Flow lines, delineated by using D8 algorithm, extracted as long, parallel lines (Fig. 4*c*). It is presented differently when using algorithms FD8 and FRho8, how it is in MFD method. On areas, where occurs changeless slope, parallel flow does not occur. Nonetheless, in many places lines demonstrating many branches of flow are formed (Fig. 4*d*).

Used algorithms do not work with determination of flow paths in areas with many drainage ditches. Faint gradient of height (minimum drop of the ditch is 0,02%, which is 0.2 m per 1 km) does not cause „disruption” in the surrounding terrain. As a result of it, determined sewage lines have compatible course with the general tendency of the terrain slope, which leads to creation of flow path's picture which does not refer to the hydrographic lines transfigured by human (Fig. 4*e*).

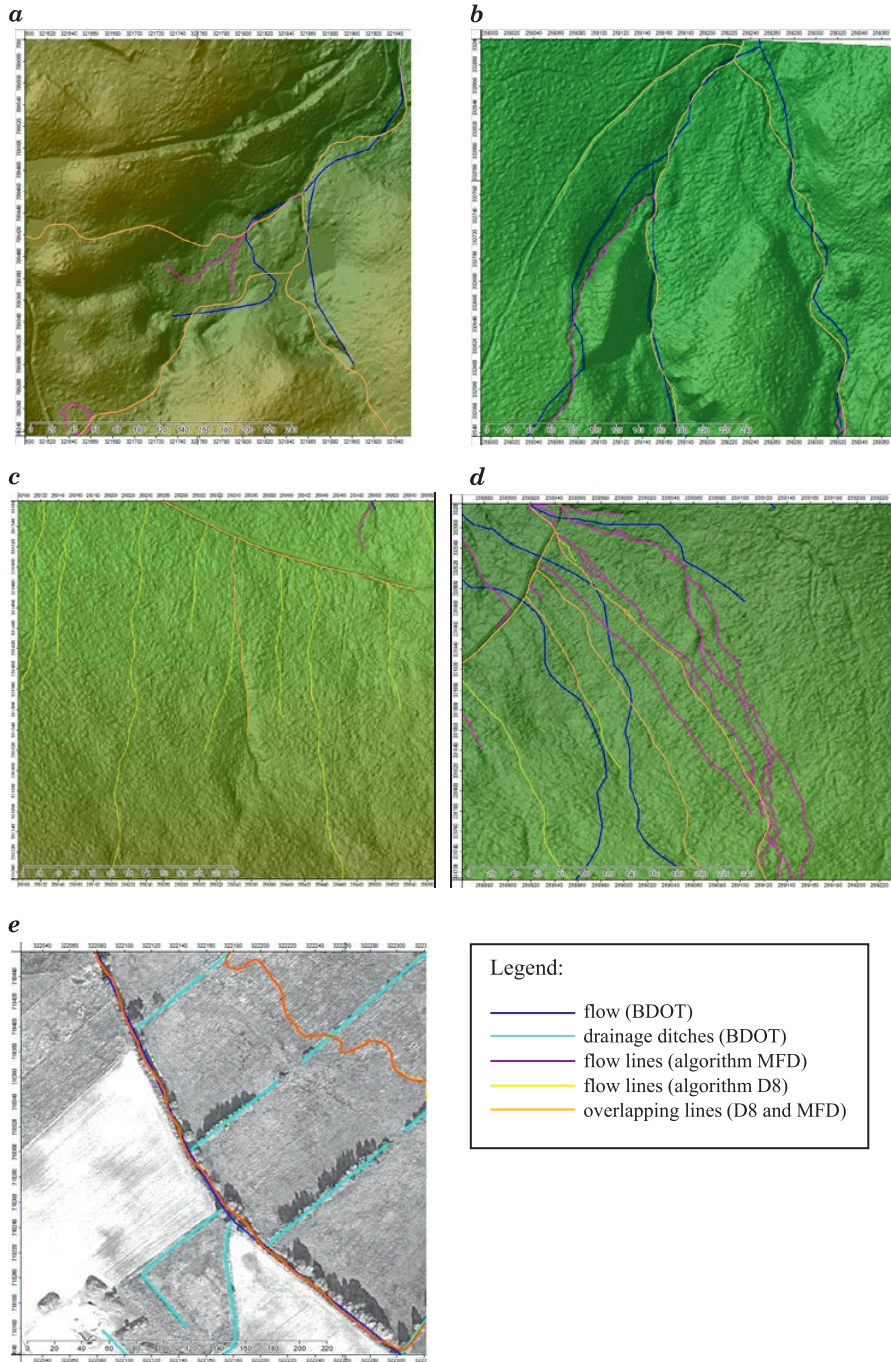


Fig. 4. Flow lines against DTM (forest areas) – sheets N-33-69-Bc-1-3 (a), M-33-44-Ca-2-3 (b, c, d) and orthophotomap – sheet N- 33-69-B-c-1-3 (e)

Analysis of delineated flow lines

This study delineating flow lines may help author to create a model of network watercourse in 3D, which will be a component of the three-dimensional Database of Topographic Objects (pol: Baza Danych Obiektów Topograficznych, BDOT10k, it is a database of topographic objects for whole Poland corresponding with detailed map with a scale of 1:10 000). Consequently, arisen flow path network was subjected to a comparative analysis with flow paths from BDOT in the next step. The source of geometry of flows from BDOT is primarily orthophotomap. In invisible places (e.g. woodland) is also acceptable acquirement of flow on the basis of other data, including topographic maps at a scale of 1:10000 (TECHNICAL GUIDELINES TBD 2008).

Drain lines delineated through the algorithms, in the next step was subjected to a comparative analysis with watercourses coming from BDOT10k, which allows to involve the following conclusions:

- On forest areas with distinct valleys accurate results were obtained for drain lines delineated by algorithms D8 and MFD (the shape and course of the watercourse is harmonized with altitude model from ALS about 95%). Drain lines' shape delivered from BDOT10k is similar, but the differences in course between the lines from BDOT10k and delineated by algorithms D8 and MDF are in some places even 20 m (Fig. 4a, b), which means that results from BDOT10k are less precise. The superior precision of lines obtained by algorithms D8 and MDF is associated with using them to extraction as source data of DTM from ALS, while the source of drain lines' geometry deriving from BDOT10k is raster of topographic map.

- For non-forest areas with visible, clear valleys were obtained to deviations to 0.5 m in watercourses' geometry (between the drain lines coming from BDOT10k (for which the source of geometry is orthophotomap) and drain lines endeared by using algorithms D8 and MFD (Fig. 4e). This means that for such areas the accuracy of the geometry designation of watercourses is satisfactory for each of used methods.

- For areas with transfigured water management (areas with drainage ditches) are marked correctly only drain lines coming from BDOT10k, of which source of data is orthophotomap (Fig. 4e). Compatibility between existing drainage ditches and watercourses generated by the algorithms is only a few percent.

- In areas with steady slope (forest areas) none of methods is not without errors (Fig. 4c, d). Correctness of watercourses' determination should be further analyzed and confronted in the fieldwork.

Conclusion

Owing the fact that for almost all over the country there is precise DTM, is worth to use automatic methods, during acquiring flow lines. It helps to obtain a more accurate shape, course and is useful for BDOT update. Generating water network based on DTM is especially applicable to those areas where is lacking of adequate visibility on orthophotomap (e.g. forest areas), then should be use different sources of data like topographic maps. It is a very important issue because in Poland forest cover is almost 30% of total land area. In connection of using raster topographic map to delineate watercourses in these areas there is a problem of the accuracy of data collection associated with raster background, its calibration and also with interpretation of introducer!!. Based on this we can say that the geometry of watercourses in forest areas in BDOT10k is approximate. Therefore it is important for the extraction of watercourses, especially in those areas, to select as source of data elevation data obtained by LIDAR technology and use the known algorithms which delineate drain lines. Thereby delineated watercourses will have acquired a more accurate geometry, consistent with the model of altitude, and time of data acquisition will be also faster.

The study also showed that delineating flow lines should not be only base on one method (JASIEWICZ 2010). To get the best model of flow network, area of research should be divided into smaller fragments, for which delineation of flow lines will be the best. The selection of algorithm (the choice of its parameters, especially the so-called threshold) has a big impact on the demarcation of flow lines. Author conducts researches using different algorithms to determine their quality for the most accurate delineation of flow lines. The results of these works will be the subject of subsequent publications.

References

- CONRAD O. 1998. *DiGem-Software for Digital Elevation Model*. Ph.D. Thesis (in German), University of Goettingen, Germany.
- COSTA-CABRAL M., BURGESS S.J. 1994. *Digital elevation model networks (DEMON): A model of flow over hillslopes for computation of contributing and dispersal areas*. Water Resources Research, 30: 1681–1692.
- FAIRFIELD J., LEYMARIE P. 1991. *Drainage networks from grid digital elevation model*. Water Resources Research, 27(5): 709–717.
- JASIEWICZ J. 2010. *Analiza topologiczna sieci drenażu w programie GRASS*. In: *GIS – woda w środowisku*. Ed. Z. Zwoliński. Bogucki Wydawnictwo Naukowe, Poznań, p. 87–119.
- LEA N.L. 1992. *An aspect driven kinematic routing algorithm*. In: *Overland Flow: Hydraulics and Erosion Mechanics*. Eds. A.J. Parsons, A.D. Abrahams. Chapman and Hall, New York, p. 147–175.
- O'CALLAGHAN J.F., MARK D.M. 1984. *The extraction of drainage networks from digital elevation data*. Computer Vision, Graphics and Image Processing, 28: 323–344.

- QUINN P.F., BEVEN K.J., CHEVALLIER P., PLANCHON O. 1991. *The prediction of hillslope flow paths for distributed hydrological modelling using digital terrain model*. Hydrological Processes, 5: 59–79.
- PARK S.J., RÜECKER G.R., AGYARE W.A., AKRAMHANOV A., KIM D., VLEK P.L.G. 2009. *Influence of Grid Cell Size and Flow Routing Algorithm on Soil-Landform Modeling*. Journal of the Korean Geographical Society, 44(2): 122–145.
- TARBOTON D.G. 1997. *A new method for the determination of flow directions and upslope areas in grid digital elevation models*. Water Resources Research, 33(2): 309–319.
- URBAŃSKI J. 2011. *GIS w badaniach przyrodniczych*. Wydawnictwo Uniwersytetu Gdańskiego, Gdańsk.
- WILSON J.P., GALLANT J.C. 2000. *Terrain analysis. Principles and applications*. John Wiley and Sons Inc., Toronto, p. 51–84.
- WOLOCK D.M., MCCABE G.J. Jr. 1995. *Comparison of Single and Multiple Flow Direction Algorithms for Computing Topographic Parameters in topmodel*. Water Resources Research, 31: 1315–1324.
- Wytyczne techniczne. Baza danych topograficznych (TBD). 2008. Wersja 1. Uzupełniona, Główny Geodeta Kraju.

Guide for Authors

Introduction

Technical Sciences is a peer-reviewed research Journal published in English by the Publishing House of the University of Warmia and Mazury in Olsztyn (Poland). Journal is published continually since 1998. Until 2010 Journal was published as a yearbook, in 2011 and 2012 it was published semiyearly. From 2013, the Journal is published quarterly in the spring, summer, fall, and winter.

The Journal covers basic and applied researches in the field of engineering and the physical sciences that represent advances in understanding or modeling of the performance of technical and/or biological systems. The Journal covers most branches of engineering science including biosystems engineering, civil engineering, environmental engineering, food engineering, geodesy and cartography, information technology, mechanical engineering, materials science, production engineering etc.

Papers may report the results of experiments, theoretical analyses, design of machines and mechanization systems, processes or processing methods, new materials, new measurements methods or new ideas in information technology.

The submitted manuscripts should have clear science content in methodology, results and discussion. Appropriate scientific and statistically sound experimental designs must be included in methodology and statistics must be employed in analyzing data to discuss the impact of test variables. Moreover there should be clear evidence provided on how the given results advance the area of engineering science. Mere confirmation of existing published data is not acceptable. Manuscripts should present results of completed works.

There are three types of papers: a) research papers (full length articles); b) short communications; c) review papers.

The Journal is published in the printed and electronic version. The electronic version is published on the website ahead of printed version of Technical Sciences.

Technical Sciences does not charge submission or page fees.

Types of paper

The following articles are accepted for publication:

Reviews

Reviews should present a focused aspect on a topic of current interest in the area of biosystems engineering, civil engineering, environmental engineering, food engineering, geodesy and cartography, information technology, mechanical engineering, materials science, production engineering etc. They should include all major findings and bring together reports from a number of sources. These critical reviews should draw out comparisons and conflicts between work, and provide an overview of the 'state of the art'. They should give objective assessments of the topic by citing relevant published work, and not merely present the opinions of individual authors or summarize only work carried out by the authors or by those with whom the authors agree. Undue speculations should also be avoided. Reviews generally should not exceed 6,000 words.

Research Papers

Research Papers are reports of complete, scientifically sound, original research which contributes new knowledge to its field. Papers should not exceed 5,000 words, including figures and tables.

Short Communications

Short Communications are research papers constituting a concise description of a limited investigation. They should be completely documented, both by reference list, and description of the experimental procedures. Short Communications should not occupy more than 2,000 words, including figures and tables.

Letters to the Editor

Letters to the Editor should concern with issues raised by articles recently published in scientific journals or by recent developments in the engineering area.

Contact details for submission

The paper should be sent to the Editorial Office, as a Microsoft Word file, by e-mail: techsci@uwm.edu.pl

Referees

Author/authors should suggest, the names, addresses and e-mail addresses of at least three potential referees. The editor retains the sole right to decide whether or not the suggested reviewers are used.

Submission declaration

After final acceptance of the manuscript, the corresponding author should send to the Editorial Office the author's declaration. Submission of an article implies that the work has not been published previously (except in the form of an abstract or as part of a published lecture or academic thesis or as an electronic preprint), that it is not under consideration for publication elsewhere, that publication is approved by all authors and tacitly or explicitly by the responsible authorities where the work was carried out, and that, if accepted, it will not be published elsewhere in the same form, in English or in any other language.

To prevent cases of ghostwriting and guest authorship, the author/authors of manuscripts is/are obliged to: (i) disclose the input of each author to the text (specifying their affiliations and contributions, i.e. who is the author of the concept, assumptions, methods, protocol, etc. used during the preparation of the text); (ii) disclose information about the funding sources for the article, the contribution of research institutions, associations and other entities.

Language

Authors should prepare the full manuscript i.e. title, abstract and the main text in English (American or British usage is accepted). Polish version of the manuscript is not required.

The file type

Text should be prepared in a word processor and saved in doc or docx file (MS Office).

Article structure

Suggested structure of the manuscript is as follows:

- Title
- Authors and affiliations
- Corresponding author
- Abstract
- Keywords
- Introduction
- Material and Methods
- Results and Discussion
- Conclusions

Acknowledgements (*optional*)
References
Tables
Figures

Subdivision – numbered sections

Text should be organized into clearly defined and numbered sections and subsections (optionally). Sections and subsections should be numbered as 1. 2. 3. then 1.1 1.2 1.3 (then 1.1.1, 1.1.2, ...). The abstract should not be included in numbering section. A brief heading may be given to any subsection. Each heading should appear on its own separate line. A single line should separate paragraphs. Indentation should be used in each paragraph.

Font guidelines are as follows:

- Title: 14 pt. Times New Roman, bold, centered, with caps
- Author names and affiliations: 12 pt. Times New Roman, bold, centered, italic, two blank line above
- Abstract: 10 pt. Times New Roman, full justified, one and a half space. Abstract should begin with the word Abstract immediately following the title block with one blank line in between. The word Abstract: 10 pt. Times New Roman, centered, indentation should be used
- Section Headings: Not numbered, 12 pt. Times New Roman, bold, centered; one blank line above
- Section Sub-headings: Numbered, 12 pt. Times New Roman, bold, italic, centered; one blank line above
- Regular text: 12 pt. Times New Roman, one and a half space, full justified, indentation should be used in each paragraph

Title page information

The following information should be placed at the first page:

Title

Concise and informative. If possible, authors should not use abbreviations and formulae.

Authors and affiliations

Author/authors' names should be presented below the title. The authors' affiliation addresses (department or college; university or company; city, state and zip code, country) should be placed below the names. Authors with the same affiliation must be grouped together on the same line with affiliation information following in a single block. Authors should indicate all affiliations with a lower-case superscript letter immediately after the author's name and in front of the appropriate address.

Corresponding author

It should be clearly indicated who will handle correspondence at all stages of refereeing and publication, also post-publication process. The e-mail address should be provided (footer, first page). Contact details must be kept up to date by the corresponding author.

Abstract

The abstract should have up to 100-150 words in length. A concise abstract is required. The abstract should state briefly the aim of the research, the principal results and major conclusions. Abstract must be able to stand alone. Only abbreviations firmly

established in the field may be eligible. Non-standard or uncommon abbreviations should be avoided, but if essential they must be defined at their first mention in the abstract itself.

Keywords

Immediately after the abstract, author/authors should provide a maximum of 6 keywords avoiding general, plural terms and multiple concepts (avoid, for example, 'and', 'of'). Author/authors should be sparing with abbreviations: only abbreviations firmly established in the field may be eligible.

Abbreviations

Author/authors should define abbreviations that are not standard in this field. Abbreviations must be defined at their first mention there. Author/authors should ensure consistency of abbreviations throughout the article.

Units

All units used in the paper should be consistent with the SI system of measurement. If other units are mentioned, author/authors should give their equivalent in SI.

Introduction

Literature sources should be appropriately selected and cited. A literature review should discuss published information in a particular subject area. Introduction should identify, describe and analyze related research that has already been done and summarize the state of art in the topic area. Author/authors should state clearly the objectives of the work and provide an adequate background.

Material and Methods

Author/authors should provide sufficient details to allow the work to be reproduced by other researchers. Methods already published should be indicated by a reference. A theory should extend, not repeat, the background to the article already dealt within the Introduction and lay the foundation for further work. Calculations should represent a practical development from a theoretical basis.

Results and Discussion

Results should be clear and concise. Discussion should explore the significance of the results of the work, not repeat them. A combined Results and Discussion section is often appropriate.

Conclusions

The main conclusions of the study may be presented in a Conclusions section, which may stand alone or form a subsection of a Results and Discussion section.

Acknowledgements

Author/authors should include acknowledgements in a separate section at the end of the manuscript before the references. Author/authors should not include them on the title page, as a footnote to the title or otherwise. Individuals who provided help during the research study should be listed in this section.

Artwork

General points

- Make sure you use uniform lettering and sizing of your original artwork
- Embed the used fonts if the application provides that option

- Aim to use the following fonts in your illustrations: Arial, Courier, Times New Roman, Symbol
- Number equations, tables and figures according to their sequence in the text
- Size the illustrations close to the desired dimensions of the printed version

Formats

If your electronic artwork is created in a Microsoft Office application (Word, PowerPoint, Excel) then please supply 'as is' in the native document format

Regardless of the application used other than Microsoft Office, when your electronic artwork is finalized, please 'Save as' or convert the images to one of the following formats (note the resolution requirements given below):

EPS (or PDF): Vector drawings, embed all used fonts

JPEG: Color or grayscale photographs (halftones), keep to a minimum of 300 dpi

JPEG: Bitmapped (pure black & white pixels) line drawings, keep to a minimum of 1000 dpi or combinations bitmapped line/half-tone (color or grayscale), keep to a minimum of 500 dpi

Please **do not**:

- Supply files that are optimized for screen use (e.g., GIF, BMP, PICT, WPG); these typically have a low number of pixels and limited set of colors
- Supply files that are too low in resolution
- Submit graphics that are disproportionately large for the content

Color artwork

Author/authors should make sure that artwork files are in an acceptable format (JPEG, EPS PDF, or MS Office files) and with the correct resolution. If, together with manuscript, author/authors submit color figures then Technical Sciences will ensure that these figures will appear in color on the web as well as in the printed version at no additional charge.

Tables, figures, and equations

Tables, figures, and equations/formulae should be identified and numbered consecutively in accordance with their appearance in the text.

Equations/mathematical and physical formulae should be presented in the main text, while tables and figures should be presented at the end of file (after References section). Mathematical and physical formulae should be presented in the MS Word formula editor.

All types of figures can be black/white or color. Author/authors should ensure that each figure is numbered and has a caption. A caption should be placed below the figure. Figure must be able to stand alone (explanation of all symbols and abbreviations used in figure is required). Units must be always included. It is noted that figure and table numbering should be independent.

Tables should be numbered consecutively in accordance with their appearance in the text. Table caption should be placed above the table. Footnotes to tables should be placed below the table body and indicated with superscript lowercase letters. Vertical rules should be avoided. Author/authors should ensure that the data presented in tables do not duplicate results described in figures, diagrams, schemes, etc. Table must be able to stand alone (explanation of all symbols and abbreviations used in table is required). Units must be always included. As above, figure and table numbering should be independent.

References

References: All publications cited in the text should be presented in a list of references following the text of the manuscript. The manuscript should be carefully checked to ensure that the spelling of authors' names and dates of publications are exactly the same in the text as in the reference list. Authors should ensure that each reference cited in the text is also present in the reference list (and vice versa).

Citations may be made directly (or parenthetically). All citations in the text should refer to:

1. Single author

The author's name (without initials, with caps, unless there is ambiguity) and the year of publication should appear in the text

2. Two authors

Both authors' names (without initials, with caps) and the year of publication should appear in the text

3. Three or more authors

First author's name followed by et al. and the year of publication should appear in the text

Groups of references should be listed first alphabetically, then chronologically.

Examples:

"... have been reported recently (ALLAN, 1996a, 1996b, 1999; ALLAN and JONES, 1995).

KRAMER et al. (2000) have recently shown..."

The list of references should be arranged alphabetically by authors' names, then further sorted chronologically if necessary. More than once reference from the same author(s) in the same year must be identified by the letters "a", "b", "c" etc., placed after the year of publication.

References should be given in the following form:

KUMBHAR B.K., AGARVAL R.S., DAS K. 1981. *Thermal properties of fresh and frozen fish*. International Journal of Refrigeration, 4(3), 143–146.

MACHADO M.F., OLIVEIRA F.A.R., GEKAS V. 1997. *Modelling water uptake and soluble solids losses by puffed breakfast cereal immersed in water or milk*. In Proceedings of the Seventh International Congress on Engineering and Food, Brighton, UK.

NETER J., KUTNER M.H., NACHTSCHEIM C.J., WASSERMAN W. 1966. *Applied linear statistical models* (4th ed., pp. 1289–1293). Irwin, Chicago.

THOMSON F.M. 1984. *Storage of particulate solids*. In M. E. Fayed, L. Otten (Eds.), *Handbook of Powder Science and Technology* (pp. 365–463). Van Nostrand Reinhold, New York.

Citation of a reference as 'in press' implies that the item has been accepted for publication.

Note that the full names of Journals should appear in reference list.

Submission checklist

The following list will be useful during the final checking of an article prior to the submission. Before sending the manuscript to the Journal for review, author/authors should ensure that the following items are present:

- Text is prepared with a word processor and saved in DOC or DOCX file (MS Office). One author has been designated as the corresponding author with contact details: e-mail address

- Manuscript has been 'spell-checked' and 'grammar-checked'

- References are in the correct format for this Journal

- All references mentioned in the Reference list are cited in the text, and vice versa

- Author/authors does/do not supply files that are too low in resolution

- Author/authors does/do not submit graphics that are disproportionately large for the content